Journal Pre-proof

A network pharmacology approach and experimental validation to investigate the anticancer mechanism of Qi-Qin-Hu-Chang formula against colitis-associated colorectal cancer through induction of apoptosis via JNK/p38 MAPK signaling pathway

Yuguang Wu, Yulai Fang, Yanan Li, Ryan Au, Cheng Cheng, Weiyang Li, Feng Xu, Yuan Cui, Lei Zhu, Hong Shen

PII: S0378-8741(23)01193-5

DOI: https://doi.org/10.1016/j.jep.2023.117323

Reference: JEP 117323

To appear in: *Journal of Ethnopharmacology*

Received Date: 1 August 2023

Revised Date: 20 September 2023

Accepted Date: 13 October 2023

Please cite this article as: Wu, Y., Fang, Y., Li, Y., Au, R., Cheng, C., Li, W., Xu, F., Cui, Y., Zhu, L., Shen, H., A network pharmacology approach and experimental validation to investigate the anticancer mechanism of Qi-Qin-Hu-Chang formula against colitis-associated colorectal cancer through induction of apoptosis via JNK/p38 MAPK signaling pathway, *Journal of Ethnopharmacology* (2023), doi: https://doi.org/10.1016/j.jep.2023.117323.

CRediT authorship contribution statement

Yuguang Wu: Conceptualization, Investigation, Methodology, Validation, Visualization, Writing – original draft. **Yulai Fang:** Investigation, Writing – review & editing. **Yanan Li:** Methodology. **Ryan Au:** Investigation, Writing – review & editing. **Cheng Cheng:** Investigation. **Weiyang Li:** Investigation. **Feng Xu:** Investigation. **Yuan Cui:** Investigation. **Lei Zhu:** Conceptualization, Project administration, Supervision, Writing – review & editing. **Hong Shen:** Conceptualization, Funding acquisition, Resources, Writing – review & editing.

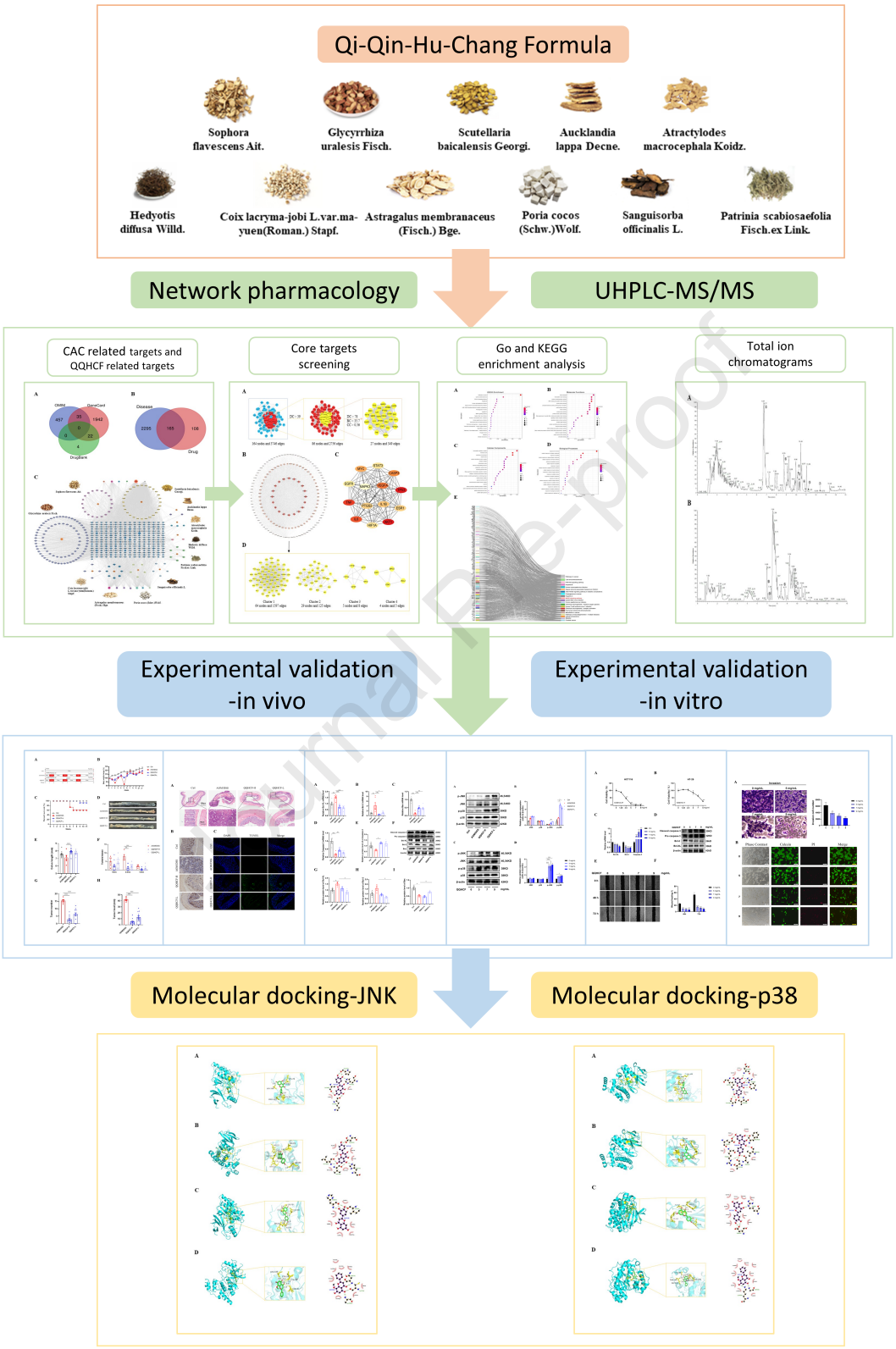

Original Article

A network pharmacology approach and experimental validation to investigate the anticancer mechanism of Qi-Qin-Hu-Chang formula against colitis-associated colorectal cancer through induction of apoptosis via JNK/p38 MAPK signaling pathway

Yuguang Wu [a, b], Yulai Fang [a], Yanan Li [a, b], Ryan Au [a, b, d], Cheng Cheng [c], Weiyang Li [a, b], Feng Xu [a, b], Yuan Cui [a, b], Lei Zhu [a, *], Hong Shen [a,*]

[a] Affiliated Hospital of Nanjing University of Chinese Medicine, Nanjing 210029, China.

[b] The First School of Clinical Medicine, Nanjing University of Chinese Medicine, Nanjing 210023, China

[c] School of Health Preservation and Rehabilitation, Nanjing University of Chinese Medicine

d Academy of Chinese Culture and Health Sciences, Oakland, CA, 94612, USA

*Correspondence should be addressed to Hong Shen; Shenhong999@njucm.edu.cn and Lei Zhu; zhulei5100@njucm.edu.cn

Abstract

Ethnopharmacological relevance: The Qi-Qin-Hu-Chang Formula (QQHCF) is a traditional Chinese medicine prescription that is clinically used at the Affiliated Hospital of Nanjing University of Chinese Medicine for the treatment of colitis-associated colorectal cancer (CAC).

Aim of the study: To evaluate the potential therapeutic effects of QQHCF on a CAC mouse model and investigate its underlying mechanisms using network pharmacology and experimental validation.

Materials and methods: The active components and potential targets of QQHCF were obtained from Traditional Chinese Medicine Systems Pharmacology (TCMSP) and herb-ingredient-targets gene network were constructed by Cytoscape 3.9.2. Target genes of CAC were obtained from GeneCards, Online Mendelian Inheritance in Man, and DrugBank database. The drug disease target protein-protein interaction (PPI) network was constructed and the core targets were visualized and identified using Cytoscape. The Metascape database was used for GO and KEGG enrichment analysis. UHPLC-MS/MS was used to further identify the active compounds in QQHCF. Subsequently, the therapeutic effects and potential mechanism of QQHCF against CAC were investigated in AOM/DSS-induced CAC mouse *in vivo*, and HT-29 and HCT116 cells *in vitro*. Finally, interactions between JNK, p38, and active ingredients were assessed by molecular docking.

Results: A total of 176 active compounds, 273 potential therapeutic targets, and 2460 CAC-related target genes were obtained. The number of common targets between QQHCF and CAC were 165. KEGG pathway analysis indicated that the MAPK signaling pathway was closely associated with CAC, which may be the potential mechanism of QQHCF against CAC. Network pharmacology and UHPLC-MS/MS analyses showed that the active compounds of QQHCF included quercetin, kaempferol, luteolin, wogonin, oxymatrine, lupanine, and baicalin. Animal experiments demonstrated that QQHCF reduced tumor load, number, and size in AOM/DSS-treated mice, and induced apoptosis in colon tissue. In vitro experiments further showed that QQHCF induced

apoptosis and inhibited cell viability, migration, and invasion in HCT116 and HT-29 cells. Notably, QQHCF activated the JNK/p38 MAPK signaling pathway both in vivo and in vitro. Molecular docking analysis revealed an ability for the main components of QQHCF and JNK/p38 to bind.

Conclusion: The present study demonstrated that QQHCF could ameliorate AOM/DSS-induced CAC in mice by activating the JNK/p38 MAPK signaling pathway. These results have important implications for the development of effective treatment strategies for CAC.

Keywords: Qi-Qin-Hu-Chang Formula, Colitis associated colorectal cancer, Network pharmacology, apoptosis, JNK/p38 MAPK signaling pathway

Introduction

Colorectal cancer (CRC) is a commonly occurring cancer and is the second highest cause of cancer-related deaths globally (Baidoun et al., 2021). Inflammatory bowel disease (IBD) is a significant contributing factor to the development of colorectal cancer (Bocchetti et al., 2021). IBD creates a chronic inflammatory environment that is not natural and supports the development of cancer. In contrast to sporadic CRC, colitis-associated colorectal cancer (CAC) follows the 'inflammation-dysplasia-carcinoma' pathway, which leads to a sequence of genetic changes (Shah and Itzkowitz, 2022). There is currently no specific medical treatment for CAC. The available evidence suggests that chemoprevention therapy with 5-aminosalicylic acid, folic acid, statins, and anti-TNF drugs can contribute to reducing the risk of CAC (Li, W. et al., 2022). However, there is still a lack of sufficient clinical trials to fully demonstrate their effectiveness in the chemoprevention of colorectal cancer.

Traditional Chinese Medicine (TCM) has the characteristics of affecting multiple targets, and having few side effects with a high curative effect (Wang et al., 2021). Studies have shown that various TCM treatments possess effective anti-tumor properties that are involved in various aspects of cancer treatment, including promoting apoptosis, inhibiting angiogenesis, and inhibiting proliferation, migration, and invasion

(Zhang et al., 2017). The results of this study indicate that TCM could be a promising therapeutic option for the prevention and treatment of cancer. In the TCM theoretical system, the etiology of CAC is deficiency of the vital-qi and the disorder of immune functions. Qi-Qin-Hu-Chang Formula (QQHCF, Patent number CN202211655092.8), is derived from Qing-Chang-Hua-Shi granule, Buqi Yunpi Decoction and Xiangshen Pill with modifications by Professor Shen. QQHCF has been utilized for the treatment of CAC at the Affiliated Hospital of Nanjing University of Chinese Medicine (Shen et al.). QQHCF is composed of 11 Chinese medicine (Table 1) : *Astragalus mongholicus* Bunge [Legume, Astragali Radix, AR], *Atractylodes macrocephala* Koidz. [Asteraceae, Atractylodis Macrocephalae Rhizoma, AMR], *Coix lacryma-jobi* L. [Gramineae, Coicis Semen, CS], *Poria cocos* (Schw.)Wolf [Polyporaceae, Porix Cocos, PC], *Sophora flavescens* Aiton [Legume, Sophorae Flavescentis Radix, SFR], *Scutellaria baicalensis* Georgi [Labiatae, Scutellariae Radix, SR], *Patrinia scabiosifolia* Link [Valerianaceae, Herba Patriniae, HP], *Scleromitrion diffusum* (Willd.) R.J.Wang [Rubiaceae Juss, Spreading Hedyotis Herb, SH], *Dolomiaea costus* (Falc.) Kasana & A.K.Pandey [Asteraceae, Aucklandiae Radix, ARs], *Sanguisorba officinalis* L. [Rosaceae Juss, Sanguisorbae Radix, SRs], *Glycyrrhiza glabra* L. [Legume, Glycyrrhizae Radix et Rhizoma, GC]. The plant name has been verified with MPNS (http://mpns.kew.org).

Chinese herbal compounds consist of four types of drugs: Sovereign, Minister, Assistant, and Courier. The Sovereign medicine serves as the primary therapeutic agent, while the Minister, Assistant, and Courier herbs provide supportive therapeutic effects. In QQHCF, AR is the Sovereign herb. AR has the action of Invigorating Qi, removing edema, expelling pus and promoting granulation, and its pharmacological activities include immune regulation, cardiovascular protection, and anticancer effects (Liu et al., 2021b; Su et al., 2021; Yang et al., 2020). AMR, HP, SH are the 'Minister drugs'. AMR strengthens Pi and induces diuresis. HP eliminates carbuncles and Clears Heat Toxins. SH promotes diuresis, Clears Heat and inhibits cancer. AMR, HP, and SH can suppress cell proliferation and induce apoptosis in cancer cells (Han et al., 2020; Huang et al., 2019; Yu et al., 2016). PC, CS, SFR, SR, and SRs are the Assistant herbs. PC and CS

can enhance the functioning of the Pi and remove Dampness. Similarly, SFR and SR are effective in eliminating Heat and Dampness from the body. Moreover, SRs are renowned for their ability to cool the blood, promote hemostasis, and facilitate the healing of sores. ARs and GC are the Courier herbs. ARs is used to regulate the flow of Qi and relieve pain, while GC is known to Invigorate the Pi, replenish Qi, and coordinate the effects of the above drugs. Both Assistant herbs and Courier herbs demonstrate anti-tumor activity (Jiang and Fan, 2020; Jo et al., 2020; Kong et al., 2021; Lee et al., 2021; Pan et al., 2023; Song et al., 2022; Zhang et al., 2019). Although QQHCF is a commonly used treatment for CAC in clinical settings, the efficacy and underlying mechanisms of its action remains unknown and requires further investigation.

In this research, we explored the active compounds, possible targets, and molecular mechanisms of QQHCF in treating CAC using network pharmacology, experimental validation, and molecular docking. We further validated our findings in both CRC cells and in a CAC mouse model.

Materials and Methods

Network pharmacology investigation of QQHCF against CAC

QQHCF herbal compounds and compound targets

The active ingredients and target proteins of QQHCF were acquired from Traditional Chinese Medicine Systems Pharmacology Database (TCMSP, https://old.tcmsp-e.com/tcmsp.php), setting the parameters of oral bioavailability (OB)⩾30% and drug-likeness (DL)⩾0.18. The target proteins' gene names were then searched in the Uniport database (https://www.uniprot.org/). Cytoscape 3.9.2 was used to create the herb-active ingredient-intersecting target network (Duan et al., 2023).

Retrieval of CAC-associated genes

Genes associated with CAC disease were retrieved from GeneCards

(https://www.genecards.org/), OMIM (https://www.omim.org/), and Drug Bank database (https://go.drugbank.com/). In these databases, genes associated with CAC were found by searching “colitis associated colorectal cancer”, with "Homo sapiens" selected as the species.

Construction of protein-protein interaction (PPI) network and selection of key targets

Draw Venn Diagram (https://bioinformatics.psb.ugent.be/webtools/Venn/) was used to visualize the intersecting targets between QQHCF and CAC.. Intersecting targets were then imported into STRING 11.5 with a required minimum network interaction score of 0.9. The PPI network was visualized and assessed with Cytoscape 3.9.2 (Ji et al., 2021). Analysis of network topology parameters of targets, including degree (DC), betweenness centrality (BC), and closeness centrality (CC), was performed using CytoNCA tools in Cytoscape software (Wang et al., 2023). The hub targets of QQHCF were selected according to the degree values that were greater than their respective medians (DC>39, BC>35.7, CC>0.56). PPI networks were filtered using the MCODE plugin in Cytoscape using a variety of cut-off values: degree=2, k-core=2, node score-0.2, and max depth=100 (Wang et al., 2022).

GO and KEGG enrichment analysis of the intersecting targets

The Metascape database (https:/metascape.org/) was used for GO (Gene Ontology) enrichment and KEGG (Kyoto Encyclopedia of Gene and Genomes) signaling pathway analysis of the main targets of QQHCF and CAC (Sun et al., 2023). The top 21 results were imported and visualized on a bioinformatics platform (http://www.bioinformatics.com.cn/) to analyze signaling pathways related to key molecular biological processes and key targets (Li, X. et al., 2022).

Molecular docking verification

Four core compounds from the QQHCF were selected through the TCMSP of the top four compounds with degree values in the PPI network for molecular docking. Mol2

molecular structure formats of QQHCF active compounds were obtained from TCMSP, imported into AutoDockTools 1.5.7 for processing, and saved in pdbqt format. The 3D structure of JNK and p38 were downloaded from the PDB protein database (https://www.rcsb.org). In Pymol, the water and organic matter molecules were replaced by hydrogen in the visualized target protein,, imported into AutoDockTools 1.5.7 for designation as a receptor, and saved as a pdbqt file (Seeliger and de Groot, 2010). AutoDockTools 1.5.7 was used for molecular docking, and the results were visualized by Pymol and LigPlus (Ye et al., 2021).

Preparation and quality control of QQHCF

The herbs in QQHCF were obtained from Jiangsu Province Hospital of TCM (Nanjing, China). The herbs were mixed (157 g total), 10-times (w/v) of distilled water was added, and the entire mixture was boiled for 40 min at 100 ℃(Hu et al., 2021). The first decoction was strained and the herbs were decocted again using the same steps. The decoctions were combined and centrifuged at 4 ℃ for 10 min. The supernatant was collected and concentrated to 66 mL for QQHCF-H group and 132 mL for QQHCF-L group using a rotary evaporator. The decoction was filtered through a 0.22 μm filter for use in cellular experiments (Hu et al., 2022).

The UHPLC-MS/MS analysis of QQHCF was performed on a SHIMADZU-LC30 UHPLC system equipped with an ACQUITY UPLC® HSS T3 column（2.1×100 mm, 1.8 μm, Waters, Milford, MA, USA) and a Thermo Scientific mass spectrometer. The sample injection volume was 4 μL, and the column was heated to 40 ℃ under a flow rate of 0.3 mL/min. The chromatography mobile phases were composed of A: 0.1% formic acid in water and B: 100% acetonitrile (ACN). The gradient elution procedure is as follows: 0-2 min, 0% B; 2-6 min, 0-48% B; 6-10 min, 48-100% B; 10-12 min 100% B; 12-12.1 min 100-0% B; 12.1-15 min, 0% B. Molecules separated by UPLC were analyzed by QE Plus mass spectrometry (Thermo Scientific). Both positive and negative-modes were applied during electrospray ionization (ESI). The ESI source conditions were as follows: Spray voltage: 3.8 kV (+) and 3.2 kV (-); Sheath Gas: 30±; Aux

Gas: 5(±); Probe Heater Temp: 350(±); S-lens RF level: 50. Raw data was analyzed using MSDIAL software for peak detection, retention time correction, and peak area extraction. Identification of compound structures were provided by Shanghai BIOPROFILE Biotechnology Co., Ltd.

Experimental verification

Reagent and Instruments

Azoxymethane (AOM, A5486) was obtained from Sigma-Aldrich (St Louis, MO, USA). Dextran sulfate sodium (DSS, MW: 36000-5000 Da) was purchased from MP Biomedicals (California, USA). Fetal Bovine Serum (FBS, C04001), DMEM (C3110) and RPMI-1640 (C3010) were obtained from VivaCell Biosciences (Shanghai, China). The following primary antibodies were used: Bcl-XL (2764), Bcl-2 (3498), Bax (2772), p38 (8690), p-p38 (9211), p-JNK (4668) provided by CST (Danvers, MA, USA). Caspase-3/Cleaved Caspase-3 (WL02117) were obtained from Wanlei (Shenyang, China). β-actin (66009-1-Ig), JNK (24164-1-AP) and the secondary antibodies HRP-conjugated Affinipure Goat Anti-Mouse IgG (H+L) (20000312), and HRP-conjugated Affinipure Goat Anti-Rabbit IgG (H+L) (20000455) were purchased from Proteintech (Rosemont, USA). Hieff@ qPCR SYBR green master mix (11201ES08) and Hifair@ III 1st Stand cDNA Synthesis Super Mix (11141ES60) were bought from YEASEN (Shanghai, China). Cell Counting Kit-8 (CCK8) was purchased from Vazyme Biotech (Nanjing, China). Transwell chambers (24-well plate, 8.0μm) were purchased from NEST (Wuxi, China). Standard OrganoGel with Phenol red was provided by Absin@ (Shanghai, China). BCA Protein Assay Kit (P0010), RIPA Lysis Buffer (Poo13B), Protease inhibitor cocktail (P1005) and Calcein/PI Cell Viability/Cytotoxicity assay kit (C2015S) were provided by Beyotime Biotechnology (Shanghai, China). Enhanced chemiluminescent (ECL) plus reagent kit was bought from Biosharp (Beijing, China). TUNEL (G1501) and Ki67 staining kits (GB111141) were provided by Servicebio Biotech (Wuhan, China).

220 **Animal experiments**

221 Animals

222 Male C57BL/6 mice (6-8 weeks old) of SPF grade were purchased from Beijing
223 SiPeiFu Biotechnology Co., Ltd (Beijing, China) and housed under SPF conditions with
224 a 12-h dark/light cycle, food and water ad libitum during the experiment. All animal
225 experiments were approved by Nanjing University of Chinese Medicine's Committee
226 for Ethics of Animal Experimentation and conducted strictly in accordance with their
227 Guidelines for Animal Experimentation.

228

229 **Establishment of CAC model and QQHCF treatment**

230 After one week of acclimation, the mice were randomly divided into four groups:
231 Ctrl group, AOM/DSS group, QQHCF-H group (23.8 g/kg/day), QQHCF-L group
232 (11.9 g/kg/day). To induce CAC, mice were given a single intraperitoneal injection (i.p.)
233 of 10 mg/kg azoxymethane (AOM), followed by seven days of regular diet with free
234 access to water. Seven days later, mice were given 2% DSS for one week and then
235 distilled water for 14 days as a recovery period. This cycle was repeated three more
236 times for 11 weeks. QQHCF (11.9, 23.8 g/kg/day) was administered by oral gavage
237 once daily. In addition, mice in the Ctrl group and AOM/DSS group were given PBS
238 by oral gavage at an equal volume. A schedule of the experiment is shown in Fig. 6A.

239

240 **H&E staining**

241 Colon tissue was fixed in 4% paraformaldehyde, embedded with paraffin, and cut
242 into 5-μm thick sections. The sections were placed on glass slides, stained with hema-
243 toxylin-eosin using standard procedures, and observed under an optical microscope.

244

245 **Immunohistochemistry (IHC) and TUNEL assay**

246 For IHC staining, tissue sections were deparaffinized and rehydrated. Antigen re-
247 trieval was performed, followed by blocking with BSA (5%, 1.5 h) and incubation with
248 primary antibodies Ki67 (1:1000, GB111141, Servicebio) at 4°C overnight. Next, slides

were incubated with secondary antibodies for 1 h and counterstained with hematoxylin for 10 min to mark the nuclei. Samples were observed by a light microscope. To detect apoptosis, a TUNEL assay was performed using the TUNEL assay kit (G1501) according to the manufacturer's protocol.

Cell culture

The human CRC cell lines HCT116 and HT-29 were provided by Nanjing University of Chinese Medicine. HCT116 were cultured in RPMI 1640 medium supplemented with 10% FBS and 1% Pen-Strep solution and HT-29 were cultured in DMEM medium supplemented with 10% FBS and 1% Pen-Strep solution. The two cell lines were cultured in an incubator at 37 ℃ with 5% CO_2.

Cell viability assay

A total of 5×10^3 HCT116 and 1×10^4 HT-29 were seeded into 96-well plate at the logarithmic phase and then treated with QQHCF at concentrations of 0, 1.25, 2.5, 5, 7, 9 mg/mL at 37 ℃ for 24 h. After 24 h of treatment, add 10 μL CCK8 to each well and incubated at 37℃ for 1 h. The absorbance at 450 nm was then recorded using a microplate reader.

Calcein/PI Cell Viability/Cytotoxicity assay

A total of 1×10^4 HT-29 were seeded into a 96-well plate and treated with QQHCF at concentrations of 0, 5, 7, and 9 mg/mL. The treatment was carried out at 37 ℃ for 24 hours. After treatment, cells were detected using Calcein/PI assay kit in accordance with the manufacturers protocols.

Wound healing assay

About 5×10^5 HT-29 cells were seeded in the 6-well plate. When cells reached 80-90% confluency, cells were scraped perpendicular to the bottom of the well with a 200 μL pipette tip and washed with PBS to remove floating cells. Different concentrations of

QQHCF (0, 5, 7, and 9 mg/mL) were added to serum-free medium in each well and incubated at 37°C for 72 h. Images were captured at 0 h, 48 h, and 72 h by using a light microscope with a magnification level of 100x. ImageJ was used for quantification and the migration rate was calculated using the following formula: Wound healing area (%)=(0 h scratch area-24 h scratch area)/0 h scratch area ×100.

Transwell migration and invasion assay

Matrigel matrix was melted in a 4°C fridge overnight, and diluted in DMEM medium at a ratio of 1:6. A total of 60 μL matrix was added to the upper Transwell chamber insert and incubated at 37°C for 4 h. HT-29 was resuspended in serum-free medium and added to the upper chamber. The lower chamber was loaded with DMEM containing 10% FBS and different concentrations of QQHCF (0, 5, 7, and 9 mg/mL). The cells were treated for 24 h. The upper chamber was removed and washed by PBS once. 600 μL 4% paraformaldehyde was added to the lower chamber for cell fixation and stained with 0.1% crystal violet solution for 15 min. The invading cells were observed by a light microscope in five random fields at a magnification of 200x and manually quantified using ImageJ software. The Transwell migration experiment followed the same steps as the Transwell invasion assay, but Matrigel was used to precoat the upper chambers.

Western blotting

Total protein was extracted from mouse colorectal tissue using RIPA buffer containing 1% PMSF. Protein quantification was performed using the BCA protein assay kit according to the manufacturer's protocol. Proteins were then separated by 10-12% SDS-PAGE, transferred to polyvinylidene difluoride membranes, blocked with 5% skimmed milk in TBS for 1 h at room temperature, and incubated with the appropriate primary antibodies (1:1000-1:2000 dilution) at 4°C overnight. The membranes were then incubated with secondary antibodies for 1 h and protein bands were detected and visualized using an ECL chromogenic substrate with a Chemiluminescence imaging

system (Bio-Rad). The expression of protein was normalized to β-actin using ImageJ software.

Real-time qRT-PCR

Total RNA was extracted from colon tissue by using Trizol reagent and reversely transcribed into cDNA using Hifair@ III 1st Strand cDNA Synthesis kits according to manufacturer's instructions. Real-time qPCR was carried out using Hieff@ qPCR SYBR green master mix with the LightCycler® 96 System (Roche, Basel, Switzerland). β-actin was used as the housekeeping gene for all reactions and gene expression wascalculated using the $^{\triangle\triangle}$Ct method = 2 ($^{\triangle}$Ct experimental – $^{\triangle}$Ct control) = $2^{-\triangle\triangle Ct}$. Primer sequences are listed in Table 6.

Statistical analysis

All statistical analyses were performed on GraphPad Prism 9.0.0. Comparisons between multiple groups were detected by one-way analysis of variance (ANOVA) tests, and comparisons between two groups were detected by t-tests. Data is expressed as the mean ± S.E.M. Values of P <0.05 were considered statistically significant.

Results

Network pharmacology-based strategy for predicting potential targets of QQHCF for treating CAC

Collection of QQHCF targets and CAC targets

Active compounds in QQHCF were compiled from the TCMSP and screened according to OB ≥ 30% and DL ≥ 0.18 conditions. A total of 176 active ingredients were obtained (Supplementary Material 1). A total of 273 therapeutic target proteins associated with 176 QQHCF-derived compounds were identified and their gene names were adjusted using the UniPort database (Supplementary Material 2). Cytoscape 3.9.2 was then used to construct the herb-component-targets gene network. As shown in (Fig. 2C), the surrounding circles represent different herbs and active compounds of QQHCF, and

the hexagons above and below represent the shared ingredients between the herbs. The blue quadrangles in the middle indicate the targets. Node degree is a measure of the number of edges attached to a node. The pharmaceutical ingredients with the highest degree values were quercetin, kaempferol, luteolin, and wogonin.

A total of 2460 CAC-related targets were collected from the GeneCards, OMIM, and DrugBank databases (Fig. 2A and Supplementary Material 3). The 165 overlapping genes between QQHCF targets and CAC targets were identified through a Venn diagram (Fig. 2B and Supplementary Material 3).

PPI network analysis and core targets screening

To identify targets that have direct or indirect interactions, the 165 overlapping genes were imported into the STRING database and a PPI network was constructed. The PPI network consisted of 164 nodes and 3746 edges (Fig. 3A). Core targets were identified based on their DC, BC, and CC values, and core and non-core target networks were constructed (Fig. 3B). The top 14 targets, ranked by degree, were shown (Fig. 3C). Table 2 shows the detailed information of the top 14 targets. Darker colors represent higher degree values. In order to delve deeper into the sub-network identified by MCODE, the targets were categorized into four distinct groups (Fig. 3D).

GO and KEGG enrichment analysis

To further investigate the function of QQHCF in CAC, we executed GO and KEGG enrichment analysis of the 165 overlapping targets. The top 21 enriched GO terms of molecular functions, cellular components, and biological processes are shown in (Fig. 4B-D and Supplementary Material 4). Molecular functions include kinase binding, transcription factor binding, protein homodimerization activity, etc. The cellular components include transcription regulatory complexes, membrane rafts, and membrane microdomains. Finally, the biological processes include responses to hormones, cellular responses to nitrogen compounds, and responses to peptides, among others. The top 21 most abundant KEGG pathways are shown and seven of these pathways

were found to be associated with the development of CAC. These include pathways in cancer, PI3K-Akt and MAPK signaling pathway, MicroRNAs in cancer, and others (Fig. 4A and E and Table 3). Additionally, we observed that 32 targets were enriched in the MAPK signaling pathway. The MAPK signaling system is crucial in cancer therapy as it enables extracellular signals to regulate various cellular functions including proliferation, differentiation, migration, and apoptosis (Anjum et al., 2022).

Identification and prediction of active compounds in QQHCF

UHPLC-MS/MS was used to identify the active ingredients in QQHCF. The representative LC-MS total ion current chromatograms (TIC) obtained in positive (ESI+) and negative ionization (ESI-) mode are shown (Fig. 5A-B). Table 4 identifies and labels the representative compounds of each herb in QQHCF, while Supplementary Material 5 provides the chemical structure and extracted ion chromatography (EIC) results. According to UHPLC-MS/MS analyses, Ammothamnine, Lupanine, and Baicalin were the three most abundant ingredients.

QQHCF alleviates AOM/DSS induced CAC in mice

To investigate the role of QQHCF in CAC, we used azoxymethane/dextran sodium sulfate (AOM/DSS) to induce CAC in mice (Fig. 6A). During the first and two DSS cycles, mice subjected to AOM/DSS treatment exhibited a greater loss of body weight compared to the Ctrl group, while QQHCF attenuated this body weight loss (Fig. 6B). Compared with the AOM/DSS group, the QQHCF group had significantly reduced survival rate and increased the colon length (Fig. 6C and E). Tumor load, number, and size were increased in AOM/DSS treated mice, whereas the QQHCF group showed fewer tumors and smaller tumor size per colon (Fig. 6D and F- H). Histological analysis of colon tissue stained with H&E showed destruction of intestinal structures, multiple adenomas and adenocarcinomas in the AOM/DSS group, which was not seen in QQHCF groups (Fig. 7A). Taken together, these results confirmed that QQHCF exerted protective effects in a CAC mouse model.

394

395 **QQHCF regulates cell proliferation and apoptosis in colon tumor tissue**

396 Cancer is characterized by aberrant regulation of both proliferation and replicative
397 immortality, which leads to unchecked cell growth (Loftus et al., 2022). Regulating the
398 balance between cell proliferation and apoptosis is of utmost importance in the context
399 of cancer development, progression, and treatment. TUNEL staining was utilized to
400 determine cell apoptosis in colon tissue, while Ki67 immunochemistry staining was
401 used to determine cell proliferation. The results indicated that the number of TUNEL-
402 positive cells in the AOM/DSS group was significantly lower than that in the control
403 group. However, this was increased in the QQHCF treatment group (Fig. 7C).
404 AOM/DSS treatment increased the number of Ki67-positive cells, while the prolifera-
405 tion level was significantly decreased in QQHCF-treated mice (Fig. 7B).

406 Next, we evaluated the expression of core regulators of the intrinsic pathway of
407 apoptosis, including Bcl-XL, Bcl-2, Bax and caspase-3 through qPCR and western blot-
408 ting (Peña-Blanco and García-Sáez, 2018). As shown in (Fig. 8A-B), the mRNA ex-
409 pression levels of Bcl-XL and Bcl-2 were significantly increased in AOM/DSS group.
410 However, after QQHCF treatment, these levels were dramatically reduced. Moreover,
411 compared with the AOM/DSS group, the mRNA expression levels of Bax and p-
412 caspase-3 were significantly increased in the QQHCF group (Fig. 8C-D). Similar re-
413 sults were confirmed by western blotting (Fig. 8E-I). Thus, the results indicated that
414 QQHCF has the potential to inhibit tumor growth by promoting tumor cell apoptosis
415 and suppressing cell proliferation.

416

417 **QQHCF treatment activates the JNK/p38 MAPK pathway *in vivo***

418 Environmental and genotoxic stresses have been shown to activate p38 and JNK
419 MAPK pathways. These two proteins are known to play crucial roles in cancer devel-
420 opment and therapy, as they regulate cell proliferation, apoptosis, and differentiation
421 (Wagner and Nebreda, 2009). Activation of the JNK/p38 MAPK signaling pathway has
422 been shown to inhibit cell proliferation and promote apoptosis. (Peluso et al., 2019).

KEGG analysis enrichment results showed that the MAPK pathway is one of the most significantly enriched pathways, therefore, the effect of QQHCF on the MAPK signaling pathway was examined. Western blotting results of colon tumor tissue indicated that QQHCF treatment increased the phosphorylation of JNK and p38 proteins but did not affect JNK and p38 expression in CAC mice (Fig.9 A-B). Taken together, these results suggest that QQHCF may affect apoptosis through the JNK/p38 MAPK signaling pathway.

QQHCF inhibits cell viability of CRC cells

To investigate the effect of QQHCF on the proliferation of CRC cell lines, we conducted CCK-8 assays. Briefly, HCT116 and HT-29 cells were incubated with various concentrations of QQHCF (0, 1.25, 2.5, 5, 7, 9 mg/mL) for 24 h and CCK-8 assays were performed. As shown in (Fig. 10A-B), QQHCF inhibited the proliferation of HCT116 and HT-29 cells in a dose-dependent manner. The IC_{50} values for QQHCF on HCT116 and HT29 cells were 2.37 mg/mL and 6.11 mg/mL, respectively, after 24 h of exposure. For subsequent analyses, we chose 1.25, 2.5, and 5 mg/mL QQHCF concentrations for HCT116 cells and 5, 7, and 9 mg/mL QQHCF concentrations for HT-29 cells. The results suggest that QQHCF has a noteworthy impact on inhibiting the growth of CRC cell lines (HCT116 and HT-29) *in vitro*. Furthermore, QQHCF exhibited no signs of toxicity in NCM460 cells (Fig. S1A).

QQHCF induces apoptosis in CRC cells

To investigate the effects of QQHCF on cell proliferation, HT-29 and HCT116 cells were exposed to varying concentrations of QQHCF (1, 2, and 5 mg/mL for HT-29 cells and 5, 7, and 9 mg/mL for HCT116 cells) for a duration of 24 h. Following exposure, RNA and protein was extracted from the cells and analyzed using qPCR and western blotting. The results suggested that the expression levels of Bcl-XL and Bcl-2 were decreased after treatment with QQHCF, whereas the expression level of p-caspase-3

was increased after treatment (Fig. 10C-D and Fig. S1B). The Calcein/PI assay demonstrated similar results (Fig. 11B). These findings strongly suggest that QQHCF is capable of inducing apoptosis in HCT116 and HT-29 cells.

QQHCF represses the migration and invasion of CRC cells

Cancer is characterized by altered tissue mechanics and metabolism, which not only affect invasion but also migration (Zanotelli et al., 2021). The objective of this study was to investigate the impact of QQHCF on the migration and invasion capabilities of CRC cell lines. The migration capacities of CRC cells were assessed using both scratch wound assay and Transwell chamber assays. Results showed that QQHCF significantly suppressed cell migration in a dose-dependent manner. After being treated with QQHCF for 24 h, the number of HT29 cells migrating to the lower chamber was inhibited by 25%, 53%, and 68% at concentrations of 5, 7, and 9 mg/mL, respectively. Moreover, wound-healing assays showed the same results (Fig. 10E-F and Fig. S1C).

The invasion capacity of CRC cells was measured using a Transwell chamber assay. The results in (Fig. 11A) demonstrate that QQHCF inhibits the invasion of CRC cells in a dose-dependent manner. Treatment of HT29 cells with 5, 7, and 9 mg/mL of QQHCF for 24 h resulted in a decrease in the number of cells invading the lower chamber by 39%, 53%, and 65%, respectively. The results obtained at the concentration of 1.25 and 2.5 mg/mL also exhibited similar outcomes (Fig. S2). Taken together, our study reveals that QQHCF exhibits suppressive effects on the migration and invasion of HT29 cells.

QQHCF activates the JNK/p38 MAPK pathway *in vitro*

As previously described, activation of the JNK/p38 MAPK pathway has been shown to accelerate cell apoptosis and inhibit cell proliferation (Ren et al., 2021). Therefore, the status of JNK/p38 MAPK pathway proteins in QQHCF treated HT29 cells was assessed by western blotting. Our findings indicate that the expression of p-JNK and p-p38 were significantly increased in HT-29 after being treated with QQHCF

for 24 h (Fig. 9C-D). This was consistent with the results of the *in vivo* study.

Predicting active compounds of QQHCF in the JNK/p38 MAPK signaling pathway

According to the PPI network results, four compounds with the highest degree of quercetin, kaempferol, luteolin, and wogonin were identified and simulated molecular docking with JNK and p38 proteins. In general, the stability of the binding conformation increases as the binding energy between the ligand and receptor decreases (Liu et al., 2021a). After analyzing the molecular docking results of JNK and p38, it was found that wogonin had the highest docking score and the lowest C-DOCKER energy (-6.72 kcal/mol). These four compounds bind well to JNK and p38 proteins, suggesting that they may be crucial in the treatment of CAC. The molecular docking results are shown in Fig. 12, Fig S3 and Table 5.

Discussion

CAC is a serious complication that arises from chronic inflammation of the colon. It is a major cause of mortality and a leading cause for colectomy. Studies conducted on Asian-Pacific populations have shown a higher prevalence of CAC as compared to western industrialized populations (Shah and Itzkowitz, 2022). This has led to extensive research in identifying the contributing factors, prevention, and treatment of CAC over the past few decades. Apart from endoscopy surveillance and chemoprevention, the standard treatment for CAC involves proctocolectomy with ileoanal anastomosis. Recent studies suggest that the preventive effect of 5-ASA and thiopurine on CAC may be diminished in cases of severe inflammation, and in some cases, these medications may even contribute to carcinogenesis instead of preventing it (Hsiao et al., 2022).

Research has shown that TCM offers distinct advantages in the treatment of cancer. TCM has the potential to enhance short-term treatment outcomes, mitigate the toxic side effects of conventional cancer treatment, improve quality of life, and ultimately prolong life expectancy (Yuan et al., 2019). As a result, TCM has become an integral

component of cancer prevention and anti-tumor therapy. According to TCM theory, the Pi is an essential organ of the human body, which is a primary source of 'Qi' and blood. Its functions not only include providing nutrients for the activities of the human body and maintaining normal metabolism, but also playing a crucial role in immune function. In TCM, the pathogenesis of CAC can be attributed to the deficiencies of the Pi and lack of Qi (Shang et al., 2023). This deficiency causes Dampness and Heat to accumulate in the colon, which damages it and leads to the development of colon ulcers. Over time, this can progress to cancer. QQHCF can strengthen the Pi and benefit Qi in the body.

Uncontrolled cell proliferation, resistance to apoptosis, invasion, and metastasis are the main features of cancer. Proliferation and apoptosis are particularly important, and research on anticancer therapy mainly focuses on the methods of inducing cancer cell apoptosis and inhibiting cancer cell proliferation (Vaghari-Tabari et al., 2021). Network pharmacology is a widely-applied approach to discovering the complex pharmacological mechanisms of TCM in treating complex diseases. In this study, we investigated the anticancer mechanism of QQHCF using a network pharmacology approach and verified the results through *in vitro* and *in vivo* experiments. In this study, we identified 165 potential anti-CAC targets of QQHCF using network pharmacology. The targets were screened based on three topological parameters: BC, CC, and DC, and 14 main targets were ultimately identified. These targets include TP53, TNFF, IL6, MAPK3, CASP3, STST3, MYC, EGFR, HIF1A, AKTA, ESR1, VEGFA, IL1β, and PTGS2, which are primarily associated with cancer, inflammation, and apoptosis. In addition, genes involved in apoptosis include BAX, CASP3, BCL2, CASP8, CASP9, CASP7, and BCL2L1. The CAC mouse model was established using AOM/DSS and treatment was QQHCF.

In vivo experiments demonstrated that QQHCF significantly reduces tumor burden, number, and size in CAC mice. To investigate the mechanism of QQHCF attenuating CAC in mice, we detected the effects of QQHCF on the proliferation and apoptosis of colon cancer cells. The study revealed that QQHCF treatment led to a reduction

in the number of cells positive for Ki67 and an increase in the number of cells positive for TUNEL. Additionally, the expression levels of apoptosis related genes Bcl-XL, Bcl-2, Bax and Caspase-3 were examined.

The results demonstrated that QQHCF treatment significantly reduced the expression levels of Bcl-XL and Bcl-2 while increasing the expression levels of Bax and p-caspase-3 in colon tissue. Similar results were obtained from *in vitro* experiments. QQHCF was found to inhibit cell proliferation and downregulate the expression levels of Bcl-XL and Bcl-2 in HCT116 and HT-29 cells. Tumor metastasis is closely linked with cell migration and invasion (Duff and Long, 2017), and QQHCF was observed to inhibit these processes in HT-29 cells. These findings suggest that QQHCF may have protective effects on CAC mice by influencing cell apoptosis and proliferation.

To investigate the mechanism of QQHCF in CAC, we conducted KEGG and GO enrichment analysis. The results of KEGG pathway analysis revealed that seven pathways were linked to CAC development, including the pathway in cancer, PI3K-Akt and MAPK signaling pathway, MicroRNAs in cancer, and others. Notably, we observed that 32 targets were enriched in the MAPK signaling pathway. The MAPK pathway plays a key role in the regulation of cellular processes such as cell proliferation, differentiation, and stress response, and is critical in cancer development. This pathway encompasses seven MAPK cascades, namely ERK1/2, JNK1/2/3, p38, ERK5, ERK3/4, ERK7/8, and NLK (Park and Baek, 2022). JNK activation has been shown to induce the mitochondrial apoptotic pathway and act as a tumor suppressor. This is due to Bcl-2-associated cell death and phosphorylation of JNK by Bim agonists. Bcl-2 and Bcl-XL induces the release of cytochrome c and activates caspases 3 and 9, leading to apoptosis (Hammouda et al., 2020). Activation of the p38 signaling cascade leads to cell cycle arrest through downregulation of G1/S or G2/M cell cycle activators (Bulavin and Fornace, 2004). Our study revealed that QQHCF increased the phosphorylation of JNK and p38 proteins in AOM/DSS induced CAC mice and CRC cells, indicating that it can activate the JNK/p38 MAPK signaling pathway both *in vivo* and *in vitro.*

In this research, we utilized network pharmacology and UHPLC-MS/MS to identify potential effective compounds in QQHCF for treating CAC. Based on network pharmacology and UHPLC-MS/MS analysis, QQHCF contains numerous pharmaceutical components such as quercetin, kaempferol, luteolin, wogonin, oxymatrine, lupanine, and baicalin. Quercetin is a flavonol, a polyphenolic flavonoid that has various pharmacological effects, such as anti-cancer, anti-inflammatory, and anti-bacterial effects. Studies have shown that quercetin can induce colon cancer cell apoptosis. In addition, kaempferol, luteolin, wogonin, oxymatrine, lupanine, and baicalin have also been shown to have anti-cancer properties (Choi et al., 2018; Kong et al., 2021; Liang et al., 2023; Nibret et al., 2021; Yoo et al., 2022; You et al., 2022). The molecules underwent a docking process, which revealed their ability to bind with JNK and p38. As a result, QQHCF improves CAC in mice by utilizing multiple compounds that work together.

Our research findings indicate that QQHCF had a protective effect against CAC in a mouse model and can trigger apoptosis in CRC cells. This effect may be attributed to the activation of the JNK/p38 MAPK pathway. However, there are still some issues to be resolved. First, more research needs to be done on its main bioactive constituents. Second, the anti-CAC mechanism of QQHCF involves multiple pharmacological effects. Several important targets and pathways have been identified in our experiments, but further pharmacological studies are needed to elucidate these complex mechanisms. Nevertheless, these findings provide a further pharmacological basis for the treatment of CAC with QQHCF and the development of QQHCF as a novel treatment for CAC.

Conclusions

In conclusion, our study results show that QQHCF can ameliorate AOM/DSS induced CAC mice and promote apoptosis in HT29 and HCT116 cells through activating the JNK/p38 MAPK signaling pathway. Additionally, *in vitro* experiments show that QQHCF inhibits the migration and invasion of HT29 cells. Our study provides a novel approach and mechanism for the treatment of CAC.

CRediT authorship contribution statement

Yuguang Wu: Conceptualization, Investigation, Methodology, Validation, Visualization, Writing – original draft. **Yulai Fang:** Investigation, Writing – review & editing. **Yanan Li:** Methodology. **Ryan Au:** Investigation, Writing – review & editing. **Cheng Cheng:** Investigation. **Weiyang Li:** Investigation. **Feng Xu:** Investigation. **Yuan Cui:** Investigation. **Lei Zhu:** Conceptualization, Project administration, Supervision, Writing – review & editing. **Hong Shen:** Conceptualization, Funding acquisition, Resources, Writing – review & editing.

Declaration of competing interest

The authors have declared no conflict of interest.

Funding

This work was supported by Postgraduate & Practice Innovation Program of Jiangsu Province (KYCX23_2134).

Acknowledgement

We greatly appreciate Shanghai BIOPROFILE Biotechnology Co., Ltd. (Shanghai, China) for UHPLC-MS/MS analysis.

References

Anjum, J., Mitra, S., Das, R., Alam, R., Mojumder, A., Emran, T.B., Islam, F., Rauf, A., Hossain, M.J., Aljohani, A.S.M., Abdulmonem, W.A., Alsharif, K.F., Alzahrani, K.J., Khan, H., 2022. A renewed concept on the MAPK signaling pathway in cancers: Polyphenols as a choice of therapeutics. Pharmacol Res 184, 106398.

Baidoun, F., Elshiwy, K., Elkeraie, Y., Merjaneh, Z., Khoudari, G., Sarmini, M.T., Gad, M., Al-Husseini, M., Saad, A., 2021. Colorectal Cancer Epidemiology: Recent Trends and Impact on Outcomes. Curr Drug Targets 22(9), 998-1009.

Bocchetti, M., Ferraro, M.G., Ricciardiello, F., Ottaiano, A., Luce, A., Cossu, A.M., Scrima, M., Leung, W.Y., Abate, M., Stiuso, P., Caraglia, M., Zappavigna, S., Yau, T.O., 2021. The Role of microRNAs in Development of Colitis-Associated Colorectal Cancer. Int J Mol Sci 22(8).

Bulavin, D.V., Fornace, A.J., Jr., 2004. p38 MAP kinase's emerging role as a tumor suppressor. Adv Cancer Res 92, 95-118.

Choi, J.B., Kim, J.H., Lee, H., Pak, J.N., Shim, B.S., Kim, S.H., 2018. Reactive Oxygen Species and p53

Mediated Activation of p38 and Caspases is Critically Involved in Kaempferol Induced Apoptosis in Colorectal Cancer Cells. J Agric Food Chem 66(38), 9960-9967.

Duan, Z.L., Wang, Y.J., Lu, Z.H., Tian, L., Xia, Z.Q., Wang, K.L., Chen, T., Wang, R., Feng, Z.Y., Shi, G.P., Xu, X.T., Bu, F., Ding, Y., Jiang, F., Zhou, J.Y., Wang, Q., Chen, Y.G., 2023. Wumei Wan attenuates angiogenesis and inflammation by modulating RAGE signaling pathway in IBD: Network pharmacology analysis and experimental evidence. Phytomedicine 111, 154658.

Duff, D., Long, A., 2017. Roles for RACK1 in cancer cell migration and invasion. Cell Signal 35, 250-255.

Hammouda, M.B., Ford, A.E., Liu, Y., Zhang, J.Y., 2020. The JNK Signaling Pathway in Inflammatory Skin Disorders and Cancer. Cells 9(4).

Han, X., Zhang, X., Wang, Q., Wang, L., Yu, S., 2020. Antitumor potential of Hedyotis diffusa Willd: A systematic review of bioactive constituents and underlying molecular mechanisms. Biomed Pharmacother 130, 110735.

Hsiao, S.W., Yen, H.H., Chen, Y.Y., 2022. Chemoprevention of Colitis-Associated Dysplasia or Cancer in Inflammatory Bowel Disease. Gut Liver 16(6), 840-848.

Hu, J., Huang, H., Che, Y., Ding, C., Zhang, L., Wang, Y., Hao, H., Shen, H., Cao, L., 2021. Qingchang Huashi Formula attenuates DSS-induced colitis in mice by restoring gut microbiota-metabolism homeostasis and goblet cell function. J Ethnopharmacol 266, 113394.

Hu, J., Tong, Y., Shen, Z., Li, Y., Cheng, C., Au, R., Xu, F., Liu, Y., Zhu, L., Shen, H., 2022. Gegen Qinlian decoction ameliorates murine colitis by inhibiting the expansion of Enterobacteriaceae through activating PPAR-γ signaling. Biomed Pharmacother 154, 113571.

Huang, S.Z., Liu, W.Y., Huang, Y., Shen, A.L., Liu, L.Y., Peng, J., 2019. Patrinia scabiosaefolia Inhibits Growth of 5-FU-Resistant Colorectal Carcinoma Cells via Induction of Apoptosis and Suppression of AKT Pathway. Chin J Integr Med 25(2), 116-121.

Ji, Y., Liu, Y., Hu, J., Cheng, C., Xing, J., Zhu, L., Shen, H., 2021. Exploring the Molecular Mechanism of Astragali Radix-Curcumae Rhizoma against Gastric Intraepithelial Neoplasia by Network Pharmacology and Molecular Docking. Evid Based Complement Alternat Med 2021, 8578615.

Jiang, Y., Fan, L., 2020. Evaluation of anticancer activities of Poria cocos ethanol extract in breast cancer: In vivo and in vitro, identification and mechanism. J Ethnopharmacol 257, 112851.

Jo, G., Kwon, M.J., Kim, J.N., Kim, B.J., 2020. Radix Sophorae Flavescentis induces apoptosis through by Caspase, MAPK Activation and ROS Signaling Pathways in 5637 Human Bladder Cancer Cells. Int J Med Sci 17(11), 1474-1481.

Kong, N., Chen, X., Feng, J., Duan, T., Liu, S., Sun, X., Chen, P., Pan, T., Yan, L., Jin, T., Xiang, Y., Gao, Q., Wen, C., Ma, W., Liu, W., Zhang, M., Yang, Z., Wang, W., Zhang, R., Chen, B., Xie, T., Sui, X., Tao, W., 2021. Baicalin induces ferroptosis in bladder cancer cells by downregulating FTH1. Acta Pharm Sin B 11(12), 4045-4054.

Lee, E.J., Kim, J.H., Kim, T.I., Kim, Y.J., Pak, M.E., Jeon, C.H., Park, Y.J., Li, W., Kim, Y.S., Choi, J.G., Chung, H.S., 2021. Sanguisorbae Radix Suppresses Colorectal Tumor Growth Through PD-1/PD-L1 Blockade and Synergistic Effect With Pembrolizumab in a Humanized PD-L1-Expressing Colorectal Cancer Mouse Model. Front Immunol 12, 737076.

Li, W., Zhao, T., Wu, D., Li, J., Wang, M., Sun, Y., Hou, S., 2022. Colorectal Cancer in Ulcerative Colitis: Mechanisms, Surveillance and Chemoprevention. Curr Oncol 29(9), 6091-6114.

Li, X., Wei, S., Niu, S., Ma, X., Li, H., Jing, M., Zhao, Y., 2022. Network pharmacology prediction and molecular docking-based strategy to explore the potential mechanism of Huanglian Jiedu

Decoction against sepsis. Comput Biol Med 144, 105389.
Liang, L., Sun, W., Wei, X., Wang, L., Ruan, H., Zhang, J., Li, S., Zhao, B., Li, M., Cai, Z., Huang, J., 2023. Oxymatrine suppresses colorectal cancer progression by inhibiting NLRP3 inflammasome activation through mitophagy induction in vitro and in vivo. Phytother Res.
Liu, J., Liu, J., Tong, X., Peng, W., Wei, S., Sun, T., Wang, Y., Zhang, B., Li, W., 2021a. Network Pharmacology Prediction and Molecular Docking-Based Strategy to Discover the Potential Pharmacological Mechanism of Huai Hua San Against Ulcerative Colitis. Drug Des Devel Ther 15, 3255-3276.
Liu, J., Nile, S.H., Xu, G., Wang, Y., Kai, G., 2021b. Systematic exploration of Astragalus membranaceus and Panax ginseng as immune regulators: Insights from the comparative biological and computational analysis. Phytomedicine 86, 153077.
Loftus, L.V., Amend, S.R., Pienta, K.J., 2022. Interplay between Cell Death and Cell Proliferation Reveals New Strategies for Cancer Therapy. Int J Mol Sci 23(9).
Nibret, E., Krstin, S., Wink, M., 2021. In vitro anti-proliferative activity of selected nutraceutical compounds in human cancer cell lines. BMC Res Notes 14(1), 18.
Pan, X., Shen, Q., Zhang, C., Zhang, X., Li, Y., Chang, Z., Pang, B., 2023. Coicis Semen for the treatment of malignant tumors of the female reproductive system: A review of traditional Chinese medicinal uses, phytochemistry, pharmacokinetics, and pharmacodynamics. Front Pharmacol 14, 1129874.
Park, H.B., Baek, K.H., 2022. E3 ligases and deubiquitinating enzymes regulating the MAPK signaling pathway in cancers. Biochim Biophys Acta Rev Cancer 1877(3), 188736.
Peluso, I., Yarla, N.S., Ambra, R., Pastore, G., Perry, G., 2019. MAPK signalling pathway in cancers: Olive products as cancer preventive and therapeutic agents. Semin Cancer Biol 56, 185-195.
Peña-Blanco, A., García-Sáez, A.J., 2018. Bax, Bak and beyond - mitochondrial performance in apoptosis. Febs j 285(3), 416-431.
Ren, Y., Lv, C., Zhang, J., Zhang, B., Yue, B., Luo, X., Yu, Z., Wang, H., Ren, J., Wang, Z., Dou, W., 2021. Alantolactone exhibits antiproliferative and apoptosis-promoting properties in colon cancer model via activation of the MAPK-JNK/c-Jun signaling pathway. Mol Cell Biochem 476(12), 4387-4403.
Seeliger, D., de Groot, B.L., 2010. Ligand docking and binding site analysis with PyMOL and Autodock/Vina. J Comput Aided Mol Des 24(5), 417-422.
Shah, S.C., Itzkowitz, S.H., 2022. Colorectal Cancer in Inflammatory Bowel Disease: Mechanisms and Management. Gastroenterology 162(3), 715-730.e713.
Shang, L., Wang, Y., Li, J., Zhou, F., Xiao, K., Liu, Y., Zhang, M., Wang, S., Yang, S., 2023. Mechanism of Sijunzi Decoction in the treatment of colorectal cancer based on network pharmacology and experimental validation. J Ethnopharmacol 302(Pt A), 115876.
Shen, H., Zhu, L., Hu, J. A traditional Chinese medicine compound composition for the treatment of colitis-associated colorectal cancer and its preparation method: CN202211655092.8 [P]. 2023-06-23.
Song, S., Zhou, J., Li, Y., Liu, J., Li, J., Shu, P., 2022. Network pharmacology and experimental verification based research into the effect and mechanism of Aucklandiae Radix-Amomi Fructus against gastric cancer. Sci Rep 12(1), 9401.
Su, H.F., Shaker, S., Kuang, Y., Zhang, M., Ye, M., Qiao, X., 2021. Phytochemistry and cardiovascular protective effects of Huang-Qi (Astragali Radix). Med Res Rev 41(4), 1999-2038.

Sun, L., Zhao, M., Li, J., Liu, J., Wang, M., Zhao, C., 2023. Exploration of the anti-liver injury active components of Shaoyao Gancao decoction by network pharmacology and experiments in vivo. Phytomedicine 112, 154717.

Vaghari-Tabari, M., Ferns, G.A., Qujeq, D., Andevari, A.N., Sabahi, Z., Moein, S., 2021. Signaling, metabolism, and cancer: An important relationship for therapeutic intervention. J Cell Physiol 236(8), 5512-5532.

Wagner, E.F., Nebreda, A.R., 2009. Signal integration by JNK and p38 MAPK pathways in cancer development. Nat Rev Cancer 9(8), 537-549.

Wang, K., Chen, Q., Shao, Y., Yin, S., Liu, C., Liu, Y., Wang, R., Wang, T., Qiu, Y., Yu, H., 2021. Anticancer activities of TCM and their active components against tumor metastasis. Biomed Pharmacother 133, 111044.

Wang, Y., Yuan, Y., Wang, W., He, Y., Zhong, H., Zhou, X., Chen, Y., Cai, X.J., Liu, L.Q., 2022. Mechanisms underlying the therapeutic effects of Qingfeiyin in treating acute lung injury based on GEO datasets, network pharmacology and molecular docking. Comput Biol Med 145, 105454.

Wang, Z.Y., Li, M.Z., Li, W.J., Ouyang, J.F., Gou, X.J., Huang, Y., 2023. Mechanism of action of Daqinjiao decoction in treating cerebral small vessel disease explored using network pharmacology and molecular docking technology. Phytomedicine 108, 154538.

Yang, B., Yang, N., Chen, Y., Zhu, M., Lian, Y., Xiong, Z., Wang, B., Feng, L., Jia, X., 2020. An Integrated Strategy for Effective-Component Discovery of Astragali Radix in the Treatment of Lung Cancer. Front Pharmacol 11, 580978.

Ye, M., Luo, G., Ye, D., She, M., Sun, N., Lu, Y.J., Zheng, J., 2021. Network pharmacology, molecular docking integrated surface plasmon resonance technology reveals the mechanism of Toujie Quwen Granules against coronavirus disease 2019 pneumonia. Phytomedicine 85, 153401.

Yoo, H.S., Won, S.B., Kwon, Y.H., 2022. Luteolin Induces Apoptosis and Autophagy in HCT116 Colon Cancer Cells via p53-Dependent Pathway. Nutr Cancer 74(2), 677-686.

You, W., Di, A., Zhang, L., Zhao, G., 2022. Effects of wogonin on the growth and metastasis of colon cancer through the Hippo signaling pathway. Bioengineered 13(2), 2586-2597.

Yu, R., Yu, B.X., Chen, J.F., Lv, X.Y., Yan, Z.J., Cheng, Y., Ma, Q., 2016. Anti-tumor effects of Atractylenolide I on bladder cancer cells. J Exp Clin Cancer Res 35, 40.

Yuan, L., Zhang, K., Zhou, M.M., Wasan, H.S., Tao, F.F., Yan, Q.Y., Feng, G., Tang, Y.S., Shen, M.H., Ma, S.L., Ruan, S.M., 2019. Jiedu Sangen Decoction Reverses Epithelial-to-mesenchymal Transition and Inhibits Invasion and Metastasis of Colon Cancer via AKT/GSK-3β Signaling Pathway. J Cancer 10(25), 6439-6456.

Zanotelli, M.R., Zhang, J., Reinhart-King, C.A., 2021. Mechanoresponsive metabolism in cancer cell migration and metastasis. Cell Metab 33(7), 1307-1321.

Zhang, W., Li, M., Du, W., Yang, W., Li, G., Zhang, C., Liang, X., Chen, H., 2019. Tissue Distribution and Anti-Lung Cancer Effect of 10-Hydroxycamptothecin Combined with Platycodonis Radix and Glycyrrhizae Radix ET Rhizoma. Molecules 24(11).

Zhang, Y., Liang, Y., He, C., 2017. Anticancer activities and mechanisms of heat-clearing and detoxicating traditional Chinese herbal medicine. Chin Med 12, 20.

Figure legend

Fig.1. Flowchart of this study.

Fig.2. Targets related to CAC and active ingredient-targets of QQHCF. **(A)** The Venn diagram of CAC therapeutic targets. **(B)** Venn diagram of CAC targets and QQHCF targets. **(C)** Herb-ingredient-targets gene network. The surrounding circles represent the different herbs and active compounds of QQHCF. The hexagons above and below represent the shared ingredients between the herbs. The blue quadrangles in the middle represent the targets.

Fig.3. The PPI network of QQHCF's targets for the treatment of CAC. **(A)** Topology screening process for PPI networks. The 27 core targets were obtained by screening 165 common targets through DC, BC, and CC. **(B)** The core and non-core target networks. **(C)** Top 14 core targets. Darker color represents higher degree value. **(D)** PPI network based on cluster analysis using the MCODE plug-in.

Fig.4. GO and KEGG enrichment analysis of 165 common targets. **(A)** KEGG pathway analysis. **(B)** Molecular function category. **(C)** Cellular component category. **(D)** Biological process category. **(E)** Sankey diagram for KEGG signaling pathway analysis. The rectangular nodes on the left represent treatment targets. The rectangular nodes on the right represent KEGG pathways. The lines represent the properties of targets and pathways.

Fig.5. Identification of active compounds in QQHCF using UHPLC-MS/MS. **(A)** QQHCF in ESI^+ mode. **(B)** QQHCF in ESI^- mode.

Fig.6. QQHCF alleviates AOM/DSS induced CAC in mice. **(A)** Schematic overview of the AOM/DSS model of colitis-associated colorectal cancer (CAC). **(B)** Percent body weight change. **(C)** Percent survival rate. **(D)** Representative colon images of CAC mice. **(E)** Colon lengths. **(F)** Tumor size distribution. **(G)** Number of tumors in colon tissue. **(H)** Tumor load in colon tissue. All data are shown in mean ± SEM (*$p<0.05$, **$p<0.01$, ***$p<0.001$).

Fig.7. QQHCF alleviates pathological changes of AOM/DSS-induced CAC mice. **(A)** Representative H&E staining of colon tissue. **(B)** Immunochemistry staining for Ki67 in colon tissue. **(C)** Immunofluorescence staining for TUNEL in colon tissue.

Fig.8. Effects of QQHCF on the colon tissue of the AOM/DSS-induced CAC mice by

789 determination of pro-apoptosis (Bax and Caspase-3), and anti-apoptosis markers (Bcl-
790 XL and Bcl-2). **(A-D)** mRNA quantification of apoptosis markers using real-time qRT-
791 PCR. **(E-I)** Determination of protein production of apoptosis markers using western
792 blot analysis. All data are shown as mean ± SEM (*p<0.05, **p<0.01, ***p<0.001).
793 **Fig.9.** QQHCF treatment activated the JNK/p38 MAPK pathway in *vivo* and v*itro*. **(A-**
794 **B)** The total (JNK and p38) and phosphorylated (p-JNK and p-p38) JNK/p38 MAPK
795 pathway proteins in colon tissue were detected by western blotting. **(C-D)** The total
796 (JNK and p38) and phosphorylated (p-JNK and p-p38) JNK/p38 MAPK pathway pro-
797 teins in HT-29 cells were detected by western blotting. All data are shown as mean ±
798 SEM (*p<0.05, **p<0.01, ***p<0.001).
799 **Fig.10.** QQHCF inhibits the cell viability and migration in HCT116 and HT-29 cells,
800 and also induces apoptosis in these cells. **(A-B)** CCK8 assays of HCT116 and HT-29
801 cells after treatment with QQHCF. **(C)** mRNA quantification of apoptosis markers us-
802 ing real-time qRT-PCR. **(D)** Determination of protein production of apoptosis markers
803 using western blot analysis. **(E)** Wound healing assays of HT-29 cells after treatment
804 with QQHCF (magnification=40x). **(F)** Quantitative histogram of the results of wound
805 healing assays. All data are shown as mean ± SEM (*p<0.05, **p<0.01, ***p<0.001).
806 **Fig.11.** QQHCF repressed the invasion and induces apoptosis in CRC cells. **(A)**
807 Transwell invasion assay of HT-29 cells after treatment with QQHCF (magnifica-
808 tion=100x). **(B)** Calcein/PI assay of HT-29 cells after treatment with QQHCF (magni-
809 fication=400x). All data are shown as mean ± SEM (*p<0.05, **p<0.01, ***p<0.001).
810 **Fig.12.** Molecular docking results of main chemical components and JNK. **(A)** Quer-
811 cetin-JNK. **(B)** Kaempterol-JNK. **(C)** luteolin-JNK. **(D)** wogonin-JNK**.**
812 **Fig.13.** Schematic diagram of QQHCF ameliorating colitis-associated colorectal cancer
813 by activating the JNK/p38 MAPK pathway (By Figdraw).
814
815 **Abbreviations:** QQHCF, Qi-Qin-Hu-Chang Formula; CAC, colitis associated colorec-
816 tal cancer; TCMSP, Traditional Chinese Medicine Systems Pharmacology; GO, gene

817 ontology; KEGG, kyoto encyclopedia of gene and genomes; PPI, protein-protein inter-
818 action; CRC, colorectal cancer; IBD, inflammatory bowel disease; TCM, Traditional
819 Chinese Medicine; OB, oral bioavailability; DL, drug-likeness; OMIM, Online Men-
820 delian Inheritance in Man; BC, betweenness centrality; CC, closeness centrality; DC,
821 degree; CAN, acetonitrile; AOM, azoxymethane; DSS, dextran sulfate sodium; TIC,
822 total ion chromatograms; EIC, extracted ion chromatography; AR, Astragali Radix;
823 AMR, Atractylodis Macrocephalae Rhizoma; CS, Coicis Semen; PC, Porix Cocos; SFR,
824 Sophorae Flavescentis Radix; SR, Scutellariae Radix; HP, Herba Patriniae; SH, Spread-
825 ing Hedyotis Herb; ARs, Aucklandiae Radix; SRs, Sanguisorbae Radix; GC, Glycyr-
826 rhizae Radix et Rhizoma.

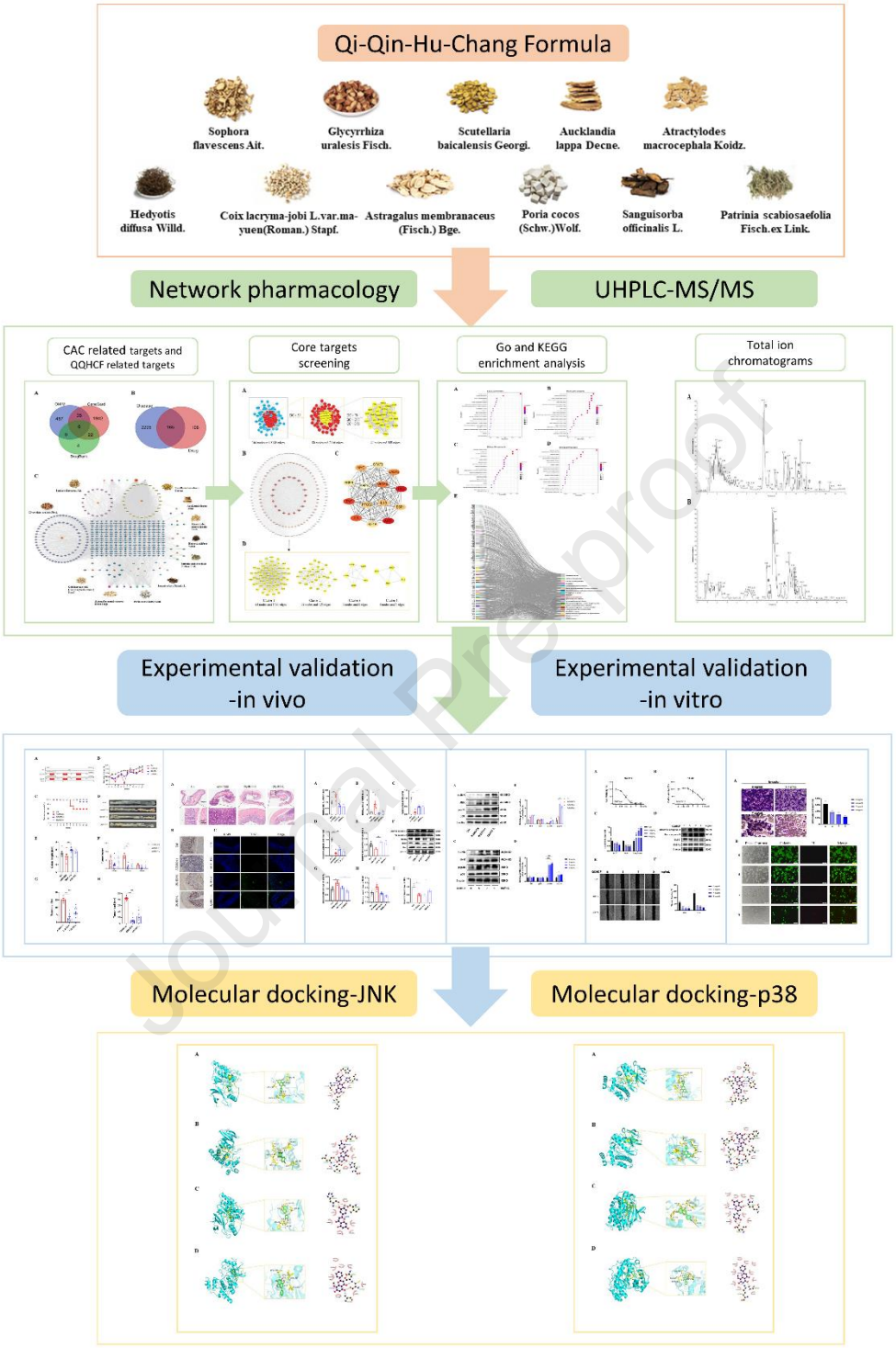
Qi-Qin-Hu-Chang Formula
Sophora flavescens Ait.
Glycyrrhiza uralesis Fisch.
Scutellaria baicalensis Georgi.
Aucklandia lappa Decne.
Atractylodes macrocephala Koidz.
Hedyotis diffusa Willd.
Coix lacryma-jobi L.var.ma-yuen(Roman.) Stapf.
Astragalus membranaceus (Fisch.) Bge.
Poria cocos (Schw.)Wolf.
Sanguisorba officinalis L.
Patrinia scabiosaefolia Fisch.ex Link.
Network pharmacology
UHPLC-MS/MS
CAC related targets and QQHCF related targets
Core targets screening
Go and KEGG enrichment analysis
Total ion chromatograms
Experimental validation -in vivo
Experimental validation -in vitro
Molecular docking-JNK
Molecular docking-p38

827

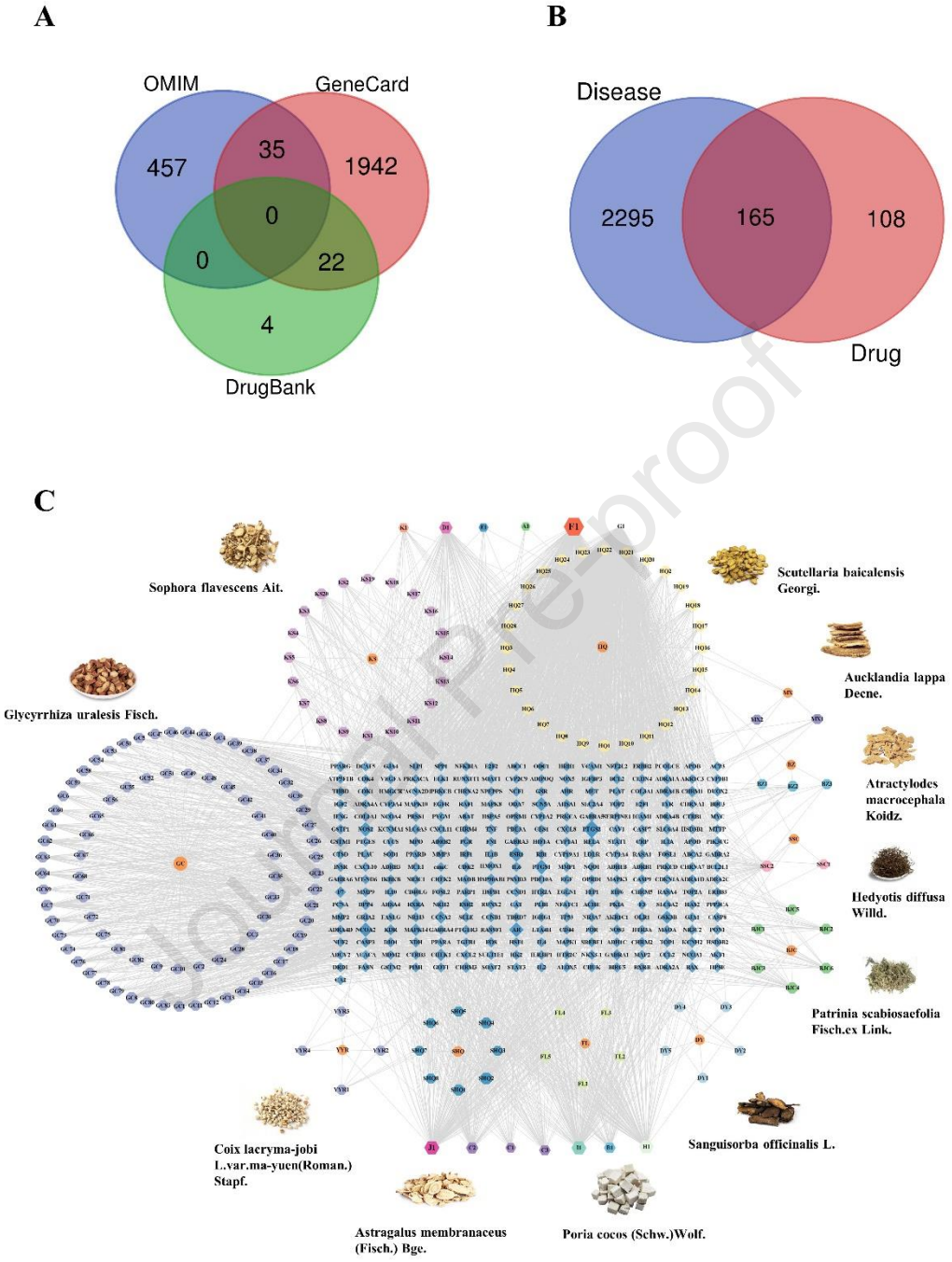
A
OMIM
GeneCard
DrugBank
457
35
1942
0
0
22
4
B
Disease
Drug
2295
165
108
C
Sophora flavescens Ait.
Scutellaria baicalensis Georgi.
Aucklandia lappa Decne.
Glycyrrhiza uralesis Fisch.
Atractylodes macrocephala Koidz.
Hedyotis diffusa Willd.
Patrinia scabiosaefolia Fisch.ex Link.
Coix lacryma-jobi L.var.ma-yuen(Roman.) Stapf.
Sanguisorba officinalis L.
Astragalus membranaceus (Fisch.) Bge.
Poria cocos (Schw.)Wolf.

828

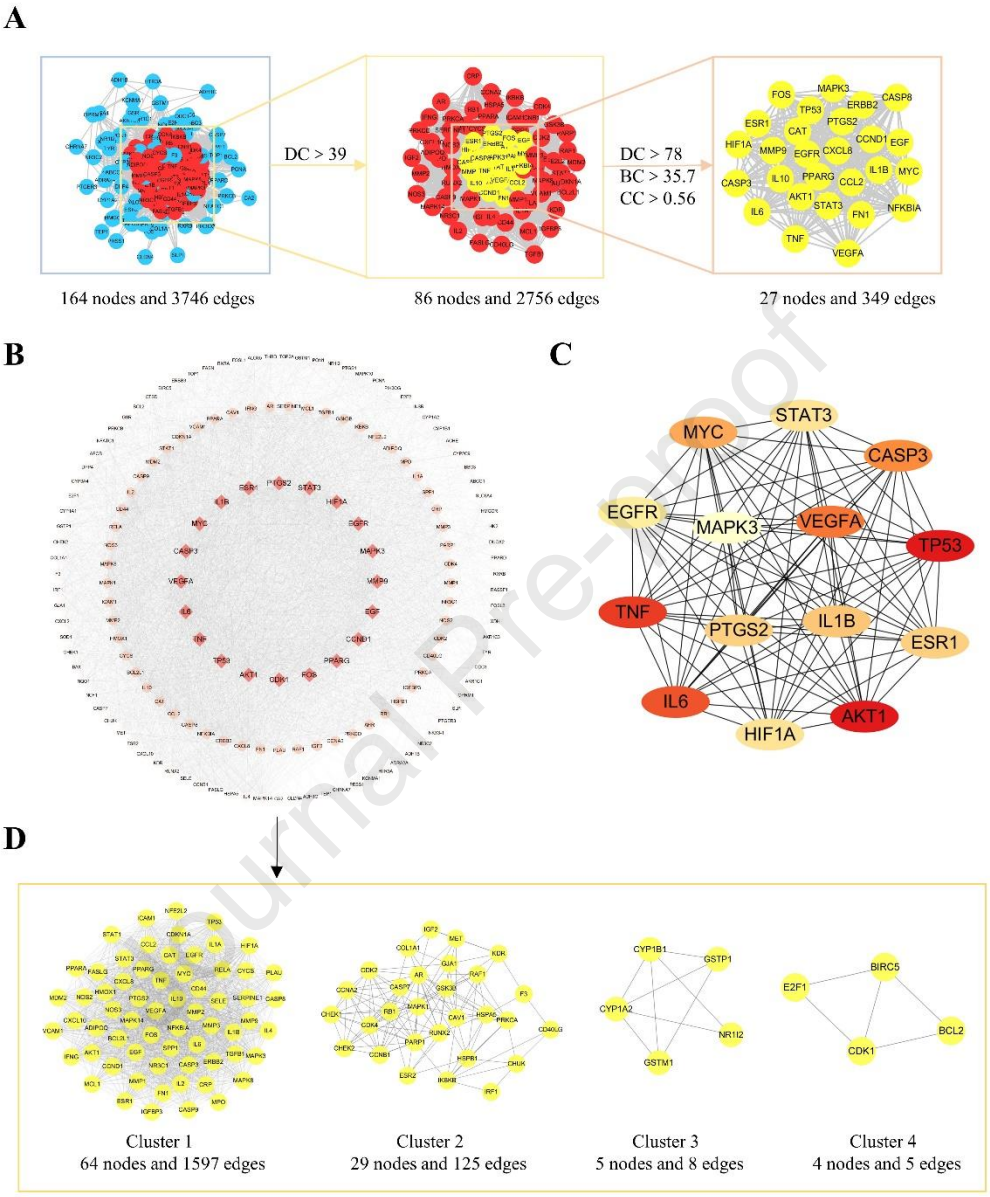
A
DC > 39
DC > 78
BC > 35.7
CC > 0.56
164 nodes and 3746 edges
86 nodes and 2756 edges
27 nodes and 349 edges
B
C
STAT3
MYC
CASP3
EGFR
MAPK3
VEGFA
TP53
TNF
PTGS2
IL1B
ESR1
IL6
AKT1
HIF1A
D
Cluster 1
64 nodes and 1597 edges
Cluster 2
29 nodes and 125 edges
Cluster 3
5 nodes and 8 edges
Cluster 4
4 nodes and 5 edges

829

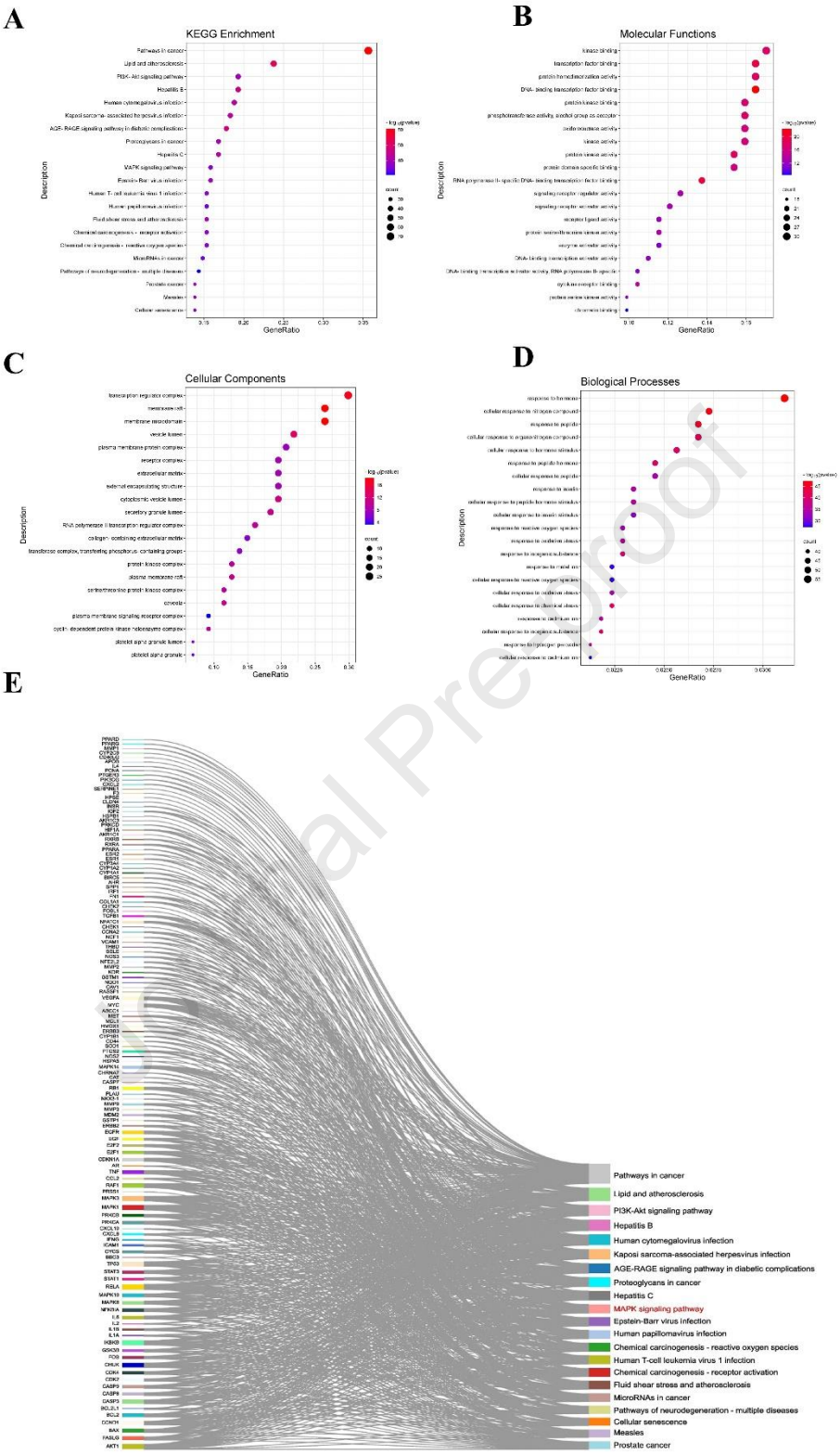

830

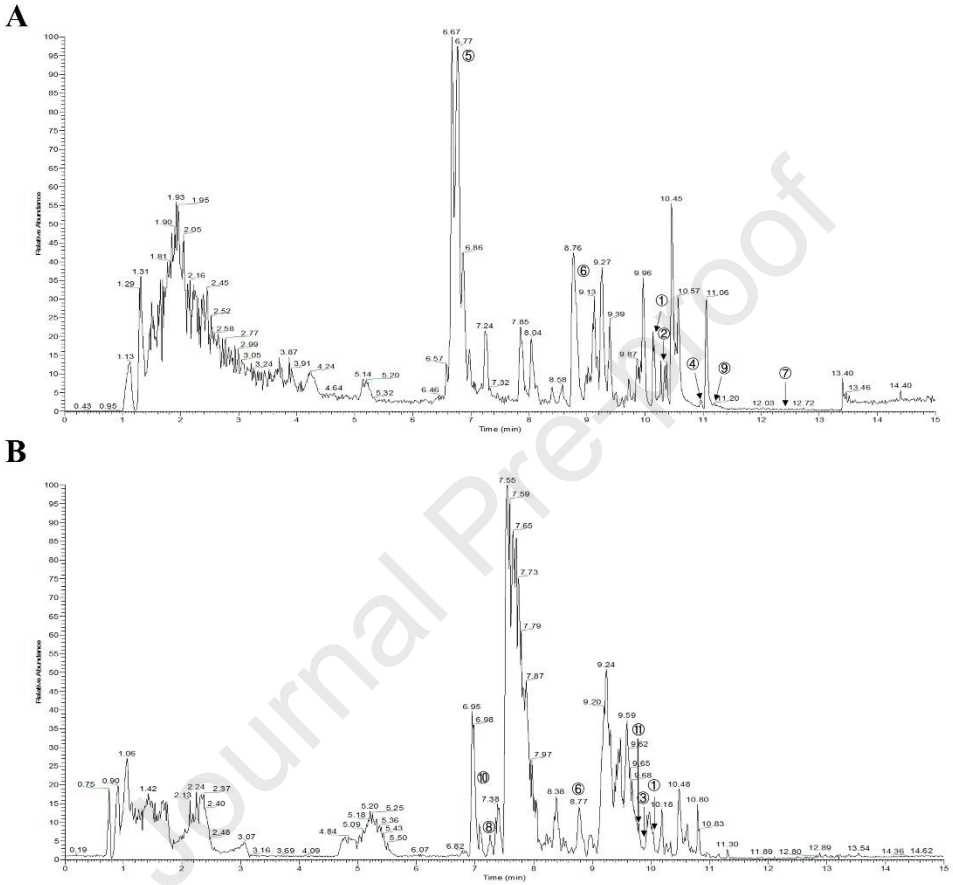

831

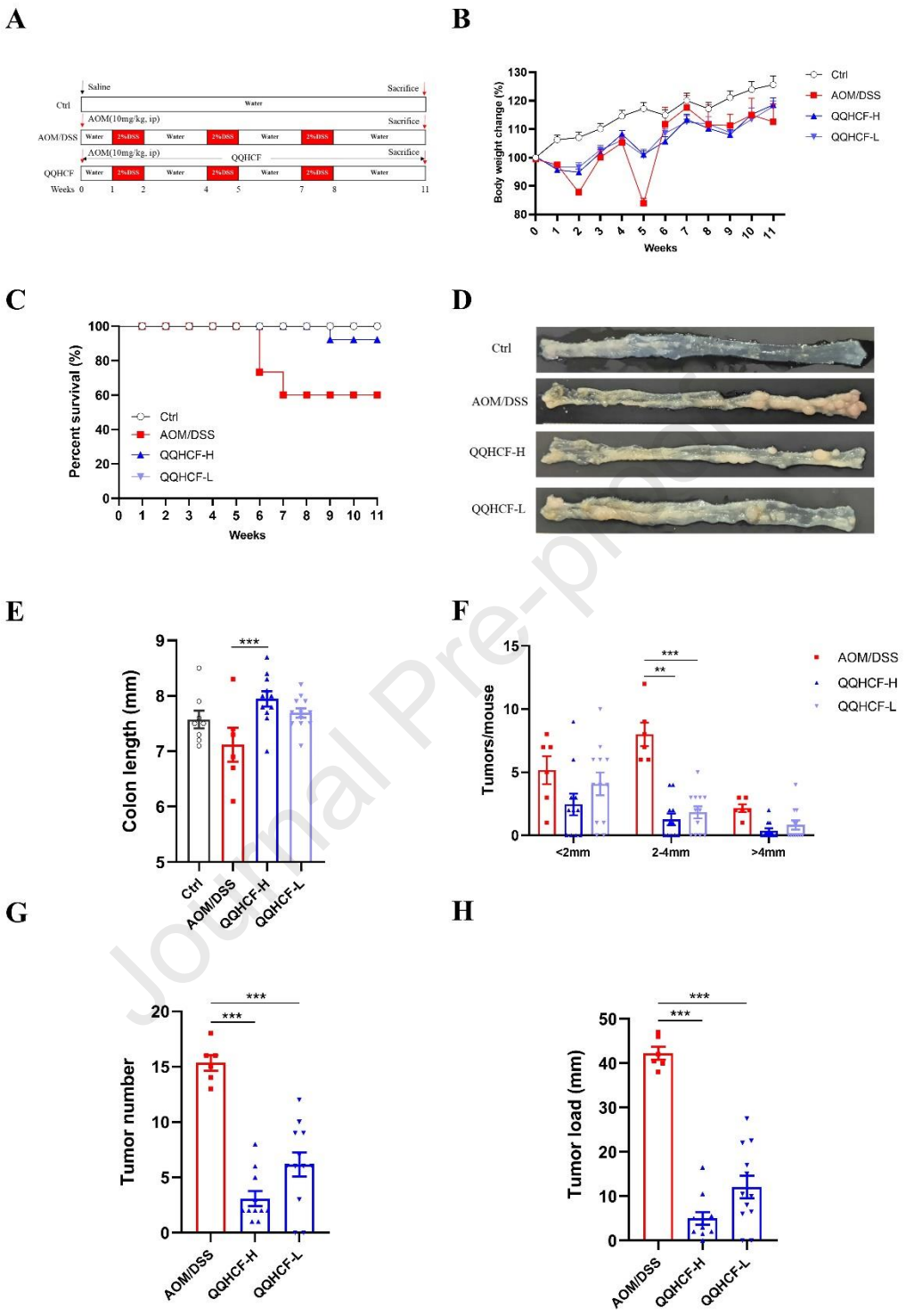
A
Saline
Sacrifice
Ctrl
Water
AOM(10mg/kg, ip)
Sacrifice
AOM/DSS
Water
2%DSS
Water
2%DSS
Water
2%DSS
Water
AOM(10mg/kg, ip)
QQHCF
Sacrifice
QQHCF
Water
2%DSS
Water
2%DSS
Water
2%DSS
Water
Weeks 0 1 2 4 5 7 8 11
B
Body weight change (%)
Weeks
Ctrl
AOM/DSS
QQHCF-H
QQHCF-L
C
Percent survival (%)
Weeks
Ctrl
AOM/DSS
QQHCF-H
QQHCF-L
D
Ctrl
AOM/DSS
QQHCF-H
QQHCF-L
E
Colon length (mm)
***
Ctrl
AOM/DSS
QQHCF-H
QQHCF-L
F
Tumors/mouse
***
**
<2mm
2-4mm
>4mm
AOM/DSS
QQHCF-H
QQHCF-L
G
Tumor number
***
***
AOM/DSS
QQHCF-H
QQHCF-L
H
Tumor load (mm)
***
***
AOM/DSS
QQHCF-H
QQHCF-L

832

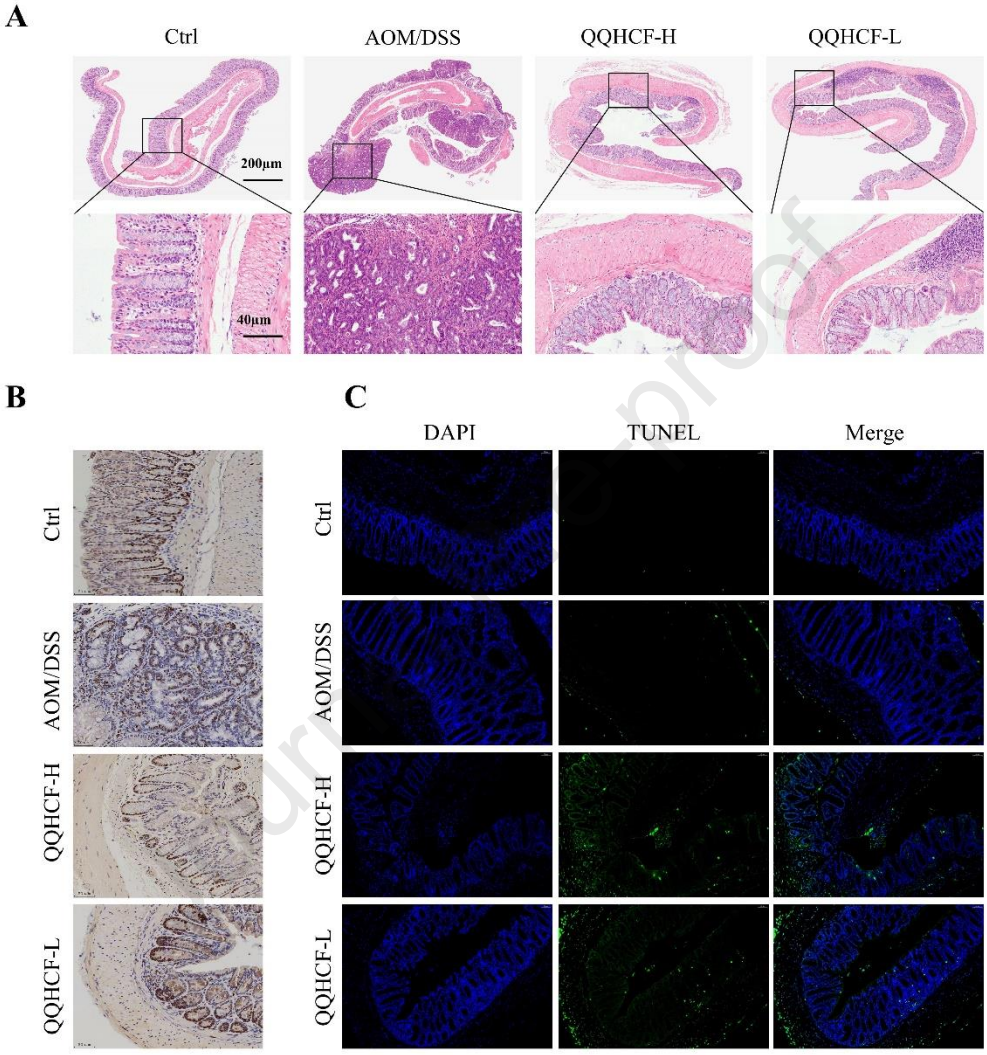
A
Ctrl
AOM/DSS
QQHCF-H
QQHCF-L
200μm
40μm
B
Ctrl
AOM/DSS
QQHCF-H
QQHCF-L
C
DAPI
TUNEL
Merge
Ctrl
AOM/DSS
QQHCF-H
QQHCF-L

833

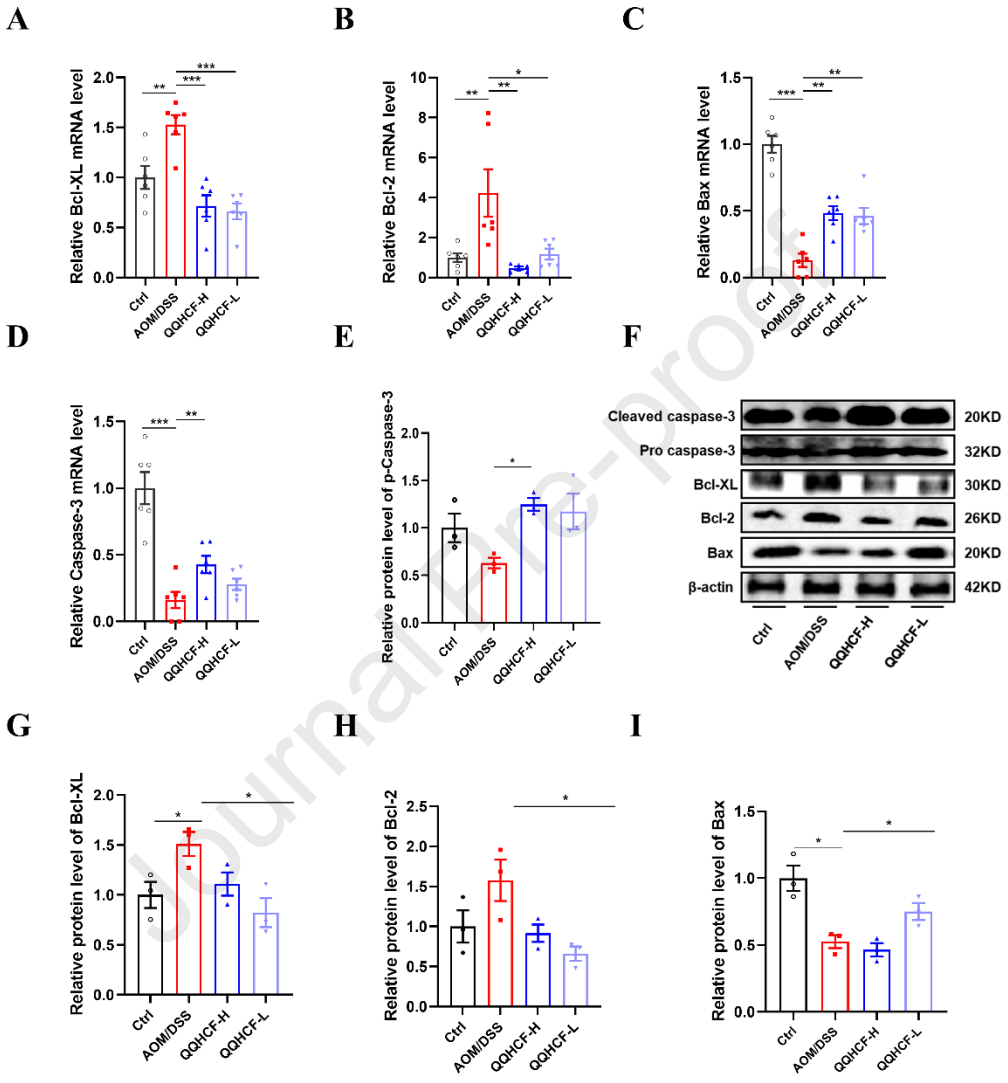
A
Relative Bcl-XL mRNA level
B
Relative Bcl-2 mRNA level
C
Relative Bax mRNA level
D
Relative Caspase-3 mRNA level
E
Relative protein level of p-Caspase-3
F
Cleaved caspase-3
Pro caspase-3
Bcl-XL
Bcl-2
Bax
β-actin
20KD
32KD
30KD
26KD
20KD
42KD
G
Relative protein level of Bcl-XL
H
Relative protein level of Bcl-2
I
Relative protein level of Bax
Ctrl
AOM/DSS
QQHCF-H
QQHCF-L

834

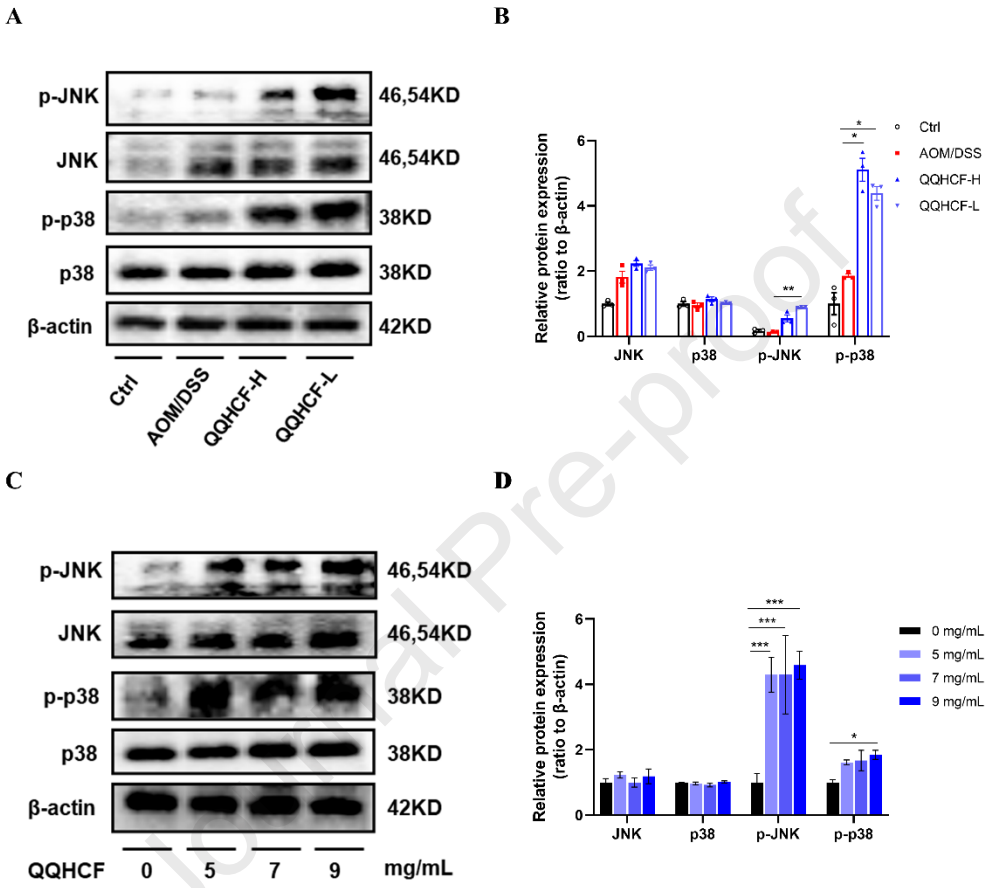
A
p-JNK
JNK
p-p38
p38
β-actin
46,54KD
46,54KD
38KD
38KD
42KD
Ctrl
AOM/DSS
QQHCF-H
QQHCF-L
B
Relative protein expression (ratio to β-actin)
Ctrl
AOM/DSS
QQHCF-H
QQHCF-L
JNK
p38
p-JNK
p-p38
C
p-JNK
JNK
p-p38
p38
β-actin
46,54KD
46,54KD
38KD
38KD
42KD
QQHCF 0 5 7 9 mg/mL
D
Relative protein expression (ratio to β-actin)
0 mg/mL
5 mg/mL
7 mg/mL
9 mg/mL
JNK
p38
p-JNK
p-p38

835

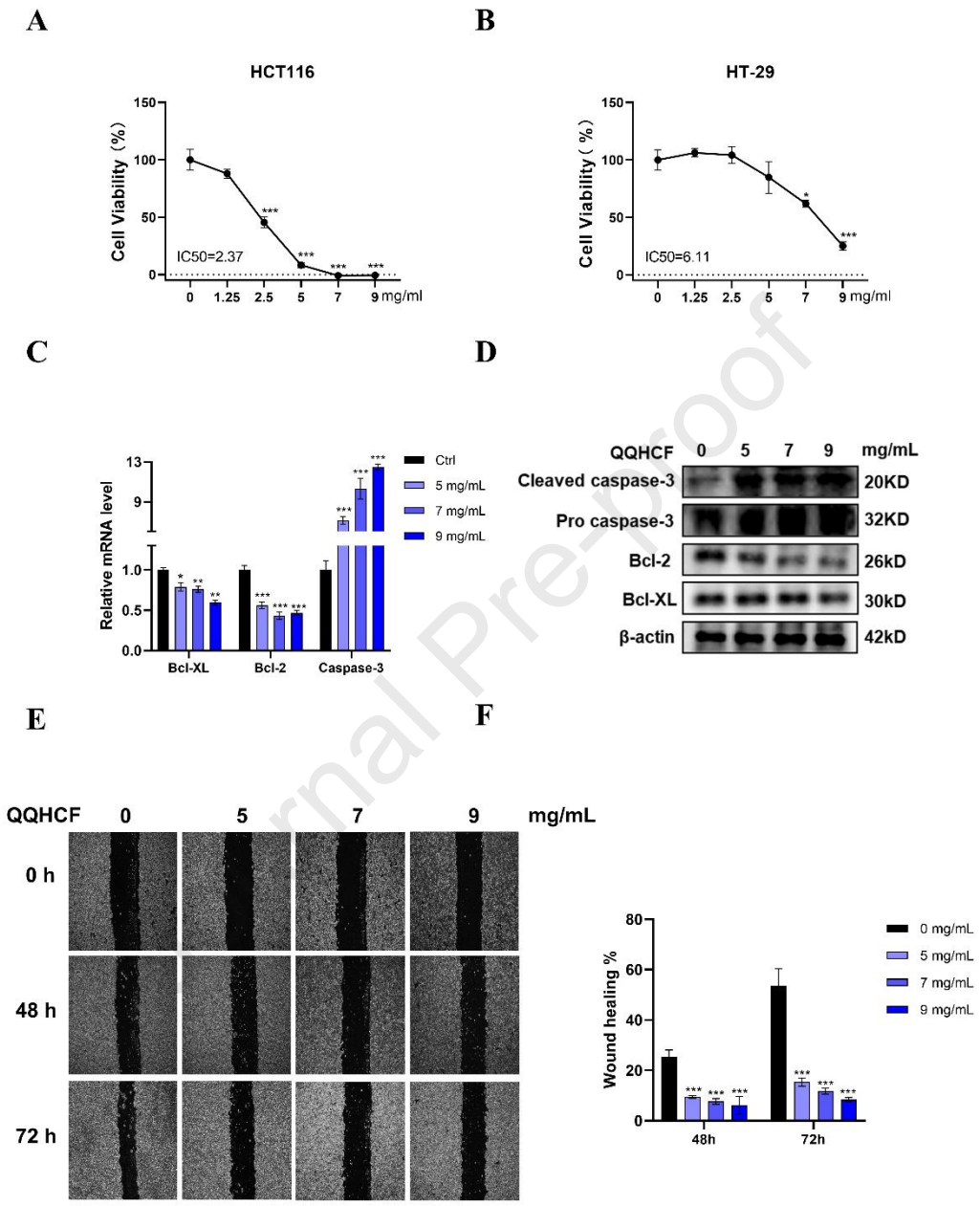
A
HCT116
Cell Viability (%)
IC50=2.37
0 1.25 2.5 5 7 9 mg/ml
B
HT-29
Cell Viability (%)
IC50=6.11
0 1.25 2.5 5 7 9 mg/ml
C
Relative mRNA level
Ctrl
5 mg/mL
7 mg/mL
9 mg/mL
Bcl-XL
Bcl-2
Caspase-3
D
QQHCF 0 5 7 9 mg/mL
Cleaved caspase-3 20KD
Pro caspase-3 32KD
Bcl-2 26kD
Bcl-XL 30kD
β-actin 42kD
E
QQHCF 0 5 7 9 mg/mL
0 h
48 h
72 h
F
Wound healing %
0 mg/mL
5 mg/mL
7 mg/mL
9 mg/mL
48h
72h

836

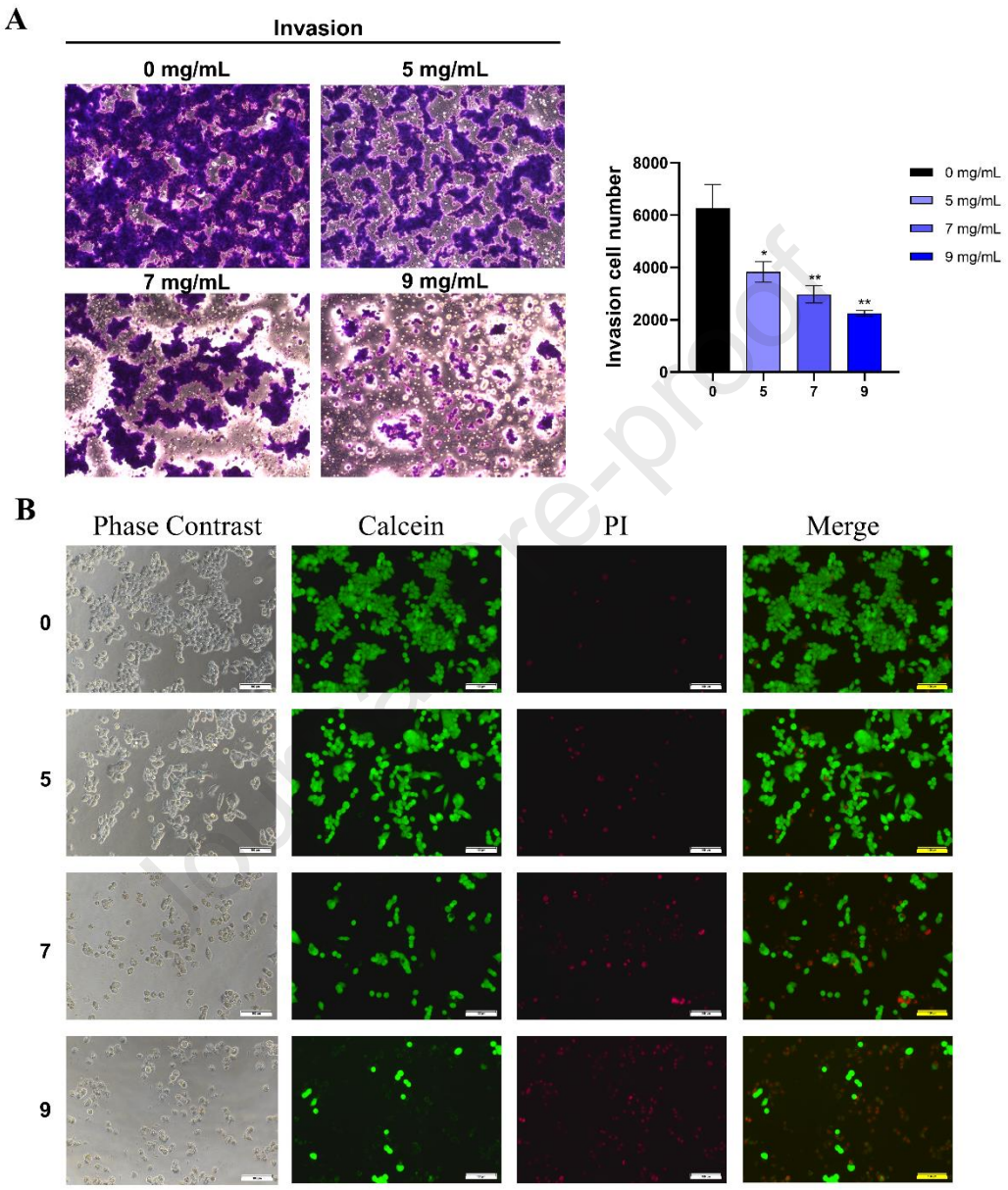
A
Invasion
0 mg/mL
5 mg/mL
7 mg/mL
9 mg/mL
Invasion cell number
8000
6000
4000
2000
0
0
5
7
9
*
**
**
0 mg/mL
5 mg/mL
7 mg/mL
9 mg/mL
B
Phase Contrast
Calcein
PI
Merge
0
5
7
9

837

A

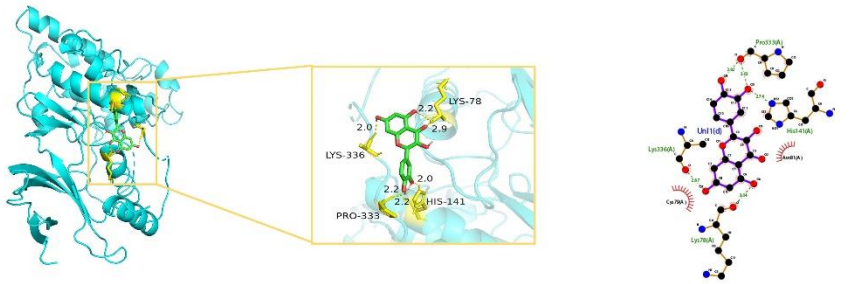

B

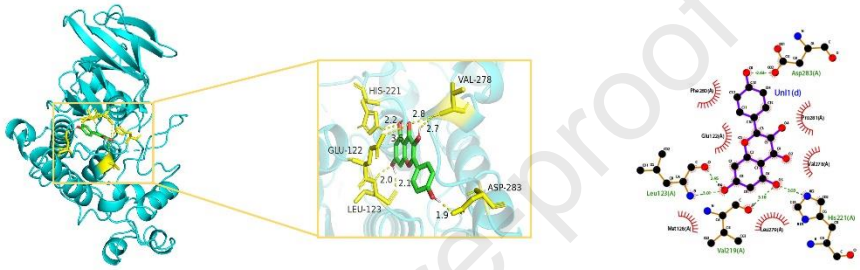

C

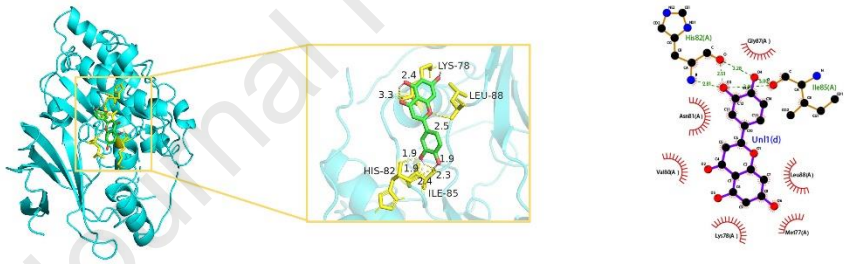

D

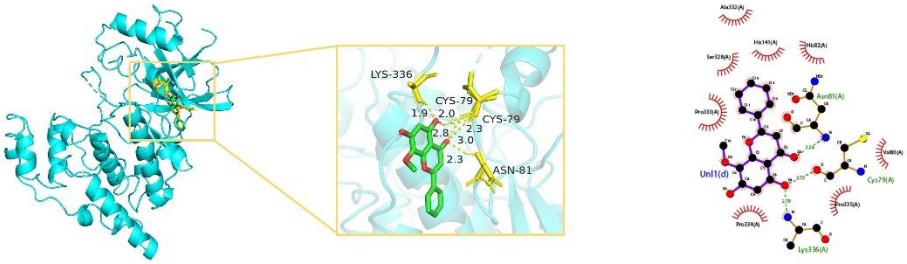

838

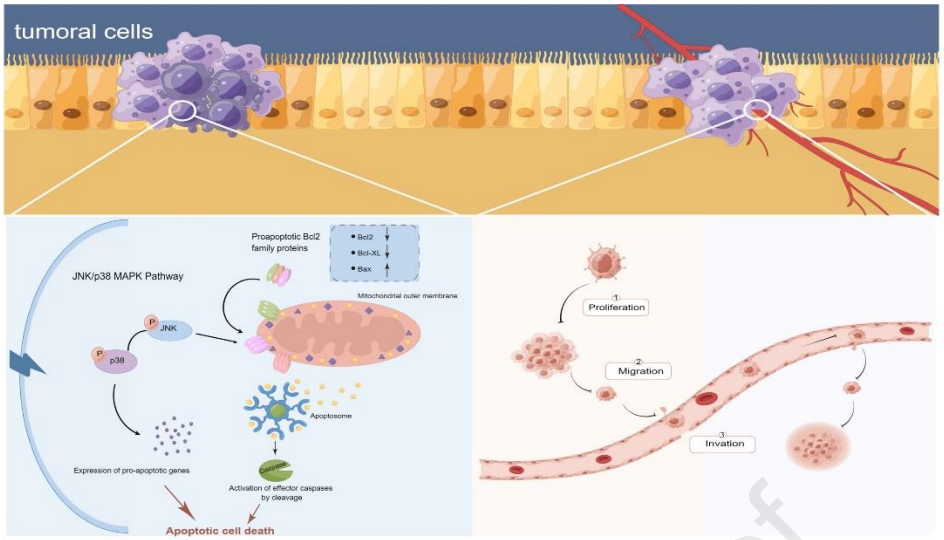

839

Table 1

Detailed information of herbs in QQHC.

Chinese name	Latin name	Part(s) used	Amount(g)
Huangqi	*Astragalus mongholicus* Bunge	roots	15
Baizhu	*Atractylodes macrocephala* Koidz.	roots	10
Yiyiren	*Coix lacryma-jobi* L.	seed kernels	30
Fuling	*Poria cocos* (Schw.)Wolf	sclerotium	15
Kushen	*Sophora flavescens* Aiton	roots	10
Huangqin	*Scutellaria baicalensis* Georgi	roots	10
Baijiangcao	*Patrinia scabiosifolia* Link	roots and rhizomes	15
Baihuasheshecao	*Scleromitrion diffusum* (Willd.) R.J.Wang	whole grass	30
Muxiang	*Dolomiaea costus* (Falc.) Kasana & A.K.Pandey	roots	6
Diyu	*Sanguisorba officinalis* L.	roots	10
Gancao	*Glycyrrhiza glabra* L.	roots and rhizomes	6

Table 2

Information of 14 core targets.

No.	UniProt ID	Gene symbol	Protein name	Degree
1	P31749	AKT1	RAC-alpha serine/threonine-protein kinase	134
2	P04637	TP53	Cellular tumor antigen p53	127
3	P01375	TNF	Tumor necrosis factor	117
4	P05231	IL6	Interleukin-6	115
5	P15692	VEGF	Vascular endothelial growth factor A	112
6	P42574	CASP3	Caspase-3	110
7	P01106	MYC	Myc proto-oncogene protein	107
8	P01584	IL1B	Interleukin-1 beta	104
9	P35354	PTGS2	Prostaglandin G/H synthase 2	103
10	P03372	ESR1	Estrogen receptor	103
11	P40763	STAT3	Signal transducer and activator of transcription 3	101
12	Q16665	HIF1A	Hypoxia-inducible factor 1-alpha	101
13	P00533	EGFR	Epidermal growth factor receptor	100
14	Q16644	MAPK3	MAP kinase-activated protein kinase 3	99

Table 3

KEGG enrichment results.

ID	Term	Count	*P*-Value
hsa05200	Pathways in cancer	72	6.05187E-82
hsa05417	Lipid and atherosclerosis	48	1.74647E-64
hsa05161	Hepatitis B	39	1.37049E-53
hsa04151	PI3K-Akt signaling pathway	39	1.80275E-39
hsa05163	Human cytomegalovirus infection	38	8.41732E-46
hsa05167	Kaposi sarcoma-associated herpesvirus infection	37	1.09519E-46
hsa04933	AGE-RAGE signaling pathway in diabetic complications	36	9.02987E-57
hsa05160	Hepatitis C	34	6.18453E-45
hsa05205	Proteoglycans in cancer	34	1.14407E-40
hsa05169	Epstein-Barr virus infection	32	1.33155E-37
hsa04010	MAPK signaling pathway	32	3.4209E-32
hsa05418	Fluid shear stress and atherosclerosis	31	2.05355E-41
hsa05166	Human T-cell leukemia virus 1 infection	31	1.19656E-34
hsa05165	Human papillomavirus infection	31	3.75572E-29
hsa05207	Chemical carcinogenesis - receptor activation	31	2.68429E-35
hsa05208	Chemical carcinogenesis - receptor activation	31	1.38374E-34
hsa05206	MicroRNAs in cancer	30	1.19043E-28
hsa05022	Pathways of neurodegeneration - multiple diseases	29	5.45384E-22
hsa05162	Measles	28	4.43686E-36

hsa05215	Prostate cancer	28	3.30241E-41
hsa04218	Cellular senescence	28	1.46216E-34

Table 4

Chemical characterization of bioactive compounds in QQHC.

NO	Name	Formula	Class	RT(min)	Intensity
①	Formononetin+-	$C_{16}H_{12}O_4$	Isoflavonoids	10.14647	30104956928
②	Atractylenolide III+	$C_{15}H_{20}O_3$	Sesquiterpene lactones	10.21618	1702038016
③	9-Oxononanoic Acid-	$C_9H_{16}O_3$	Medium-chain fatty acids	9.901733	449050272
④	Poricoic Acid B+	$C_{30}H_{44}O_5$	Triterpenoids	10.9162	334360512
⑤	Ammothamnine+	$C_{15}H_{24}N_2O_2$	Matrine alkaloids	6.765983	3.45563E+11
⑥	Baicalin+/-	$C_{21}H_{18}O_{11}$	Flavonoid O-glycosides	8.773483	18628802560
⑦	Oleanolic Acid+	$C_{30}H_{48}O_3$	Triterpenoids	12.40875	79542048
⑧	Asperuloside-	$C_{15}H_{18}O_2$	Glycosyl compounds	7.353567	1056839552
⑨	Dehydrocostus Lactone+	$C_{15}H_{20}O_2$	Sesquiterpene lactones	11.12615	5934508032
⑩	Gallic Acid-	$C_7H_6O_5$	Hydroxybenzoic acid derivatives	7.031367	2894515712
⑪	Glycyrrhizin-	$C_{42}H_{62}O_{16}$	Triterpene glycosides	9.718384	5782703104

Table 5

Details of targets and compounds for molecular docking.

Target	Target (PDB ID)	Target Structure	Compound	Affinity (kcal/mol)
JNK	3ELJ	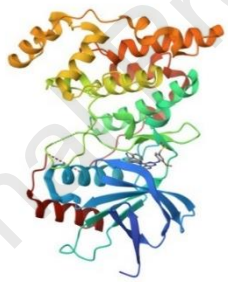	quercetin	-5.04
			Kaempterol	-4.94
			luteolin	-5.63
			wogonin	-5.81
P38	1R3C	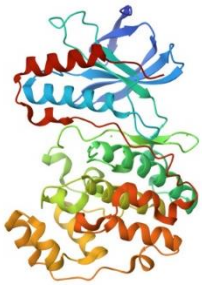	quercetin	-4.63
			Kaempterol	-5.02
			luteolin	-5.62
			wogonin	-6.72

Table 6

Primer sequence.

Gene	Primer	Sequence (5’-3’)
Mouse-β-actin	F	CTCATGAAGATCCTGACCGAG
	R	AGTCTAGAGCAACATAGCACAG
Human-GAPDH	F	GAGAAGGCTGGGGCTCATTT
	R	AGTGATGGCATGGACTGTGG
Human-Bcl-2	F	GGGTGAACTGGGGGAGGATT
	R	CAGCCCAGACTCACATCACCAA
Human-Bcl-XL	F	TCCCCATGGCAGCAGTAAAG
	R	AGGTAAGTGGCCATCCAAGC
Human-Caspase-3	F	GTCGATGCAGCAAACCTCAG
	R	CCACGGCAGGCCTGAATAAT

Mouse-Bcl-2	F	GAGTTCGGTGGGGTCATGTG
	R	CTTCAGAGACAGCCAGGAGAAA
Mouse-Bcl-XL	F	ATTCCCATGGCAGCAGTGAA
	R	CCGCCAAAGGAGAAAAAGGC
Mouse-Bax	F	GATCCAAGACCAGGGTGGC
	R	CTTCCAGATGGTGAGCGAGG
Mouse-Caspase-3	F	GTCATCTCGCTCTGGTACGG
	R	CACACACACAAAGCTGCTCC

Highlights

- **We firstly conducted bioinformatic methods and animal experiments to illuminate the anti-CAC mechanism of QQHCF.**
- **QQHCF can ameliorate AOM/DSS-induced CAC mice.**
- **QQHCF can promote apoptosis in HT29 and HCT116 cells.**
- **QQHCF can inhibit the migration and invasion of HT29 cells.**
- **QQHCF can activate the JNK/p38 MAPK signaling pathway in vitro and vivo.**
- **Our study provides a novel approach and mechanism for the treatment of CAC.**

Conflict of Interest

Declarations of interest: none

All authors declare that they have no conflicts of interest.